Export fluxes in a naturally iron-fertilized area of the Southern Ocean: seasonal dynamics of particulate organic carbon export from a moored sediment trap (part 1).

M. Rembauville[1,2] , I. Salter[1,2,3] , N. Leblond[4,5] , A. Gueneugues[1,2] and S. Blain[1,2]

[1] Sorbonne Universités, UPMC Univ Paris 06, UMR 7621, LOMIC, Observatoire Océanologique, Banyuls-sur-Mer, France.

[2] CNRS, UMR 7621, LOMIC, Observatoire Océanologique, Banyuls-sur-Mer, France.

[3] Alfred-Wegener-Institute for Polar and Marine research, Bremerhaven, Germany.

[4]Sorbonne Universités, UPMC Univ Paris 06, LOV, UMR 7093, Observatoire Océanologique, Villefranche-sur-Mer, France

[5]CNRS-INSU, LOV, UMR 7093, Observatoire Océanologique, Villefranche-sur-Mer, France

Correspondance to: M. Rembauville (rembauville@obs-banyuls.fr).

Abstract

A sediment trap moored in the naturally iron-fertilized Kerguelen plateau in the Southern Ocean provided an annual record of particulate organic carbon and nitrogen fluxes at 289 m. At the trap deployment depth current speeds were typically low (~10 cm s^{-1}) and primarily tidal-driven (M2 tidal component). Although advection was weak, the sediment trap may have been subject to hydrodynamical and biological (swimmer feeding on trap funnel) biases. Particulate organic carbon (POC) flux was generally low (<0.5 mmol m^{-2} d^{-1}) although two episodic export events (<14 days) of 1.5 mmol m^{-2} d^{-1} were recorded. These increases in flux occurred with a 1-month time lag from peaks in surface chlorophyll and together accounted for approximately 40 % of the annual flux budget. The annual POC flux of 98.2±4.4 mmol m^{-2} y^{-1} was low considering the shallow deployment depth, but comparable to independent

estimates made at similar depths (~300 m) over the plateau, and to deep-ocean (>2 km) fluxes measured from similarly productive iron-fertilized blooms. Although undertrapping cannot be excluded in shallow moored sediment trap deployment, we hypothesize that grazing pressure, including mesozooplankton and mesopelagic fishes, may be responsible for the low POC flux beneath the base of the winter mixed layer. The importance of plankton community structure in controlling the temporal variability of export fluxes is addressed in a companion paper.

1 Introduction

The biological carbon pump is defined as the downward transfer of biologically fixed carbon from the ocean surface to the ocean interior (Volk and Hoffert, 1985). Global estimates of Particulate Organic Carbon (POC) export cluster between 5 Pg C y^{-1} (Moore et al., 2004; Lutz et al., 2007; Honjo et al., 2008; Henson et al., 2011; Lima et al., 2014) and 10 Pg C y^{-1} (Laws et al., 2000; Schlitzer, 2004; Gehlen et al., 2006; Boyd and Trull, 2007; Dunne et al., 2007; Laws et al., 2011). The physical transfer of dissolved inorganic carbon to the ocean interior during subduction of water masses is two orders of magnitude higher (> 250 Pg C y^{-1}, Karleskind et al., 2011; Levy et al., 2013). The global ocean represents a net annual CO_2 sink of 2.5 Pg C y^{-1} (Le Quéré et al., 2013), slowing down the increase of the atmospheric CO_2 concentration resulting from anthropogenic activity. Although the Southern Ocean (south of 44°S) plays a limited role in the net air-sea CO_2 flux (Lenton et al., 2013), it is a key component of the global anthropogenic CO_2 sink representing one third the global oceanic sink (~1 Pg C y^{-1}) while covering 20 % of its surface (Gruber et al., 2009). The solubility pump is considered as the major component of this sink, whereas the biological carbon pump is considered to be inefficient in the Southern Ocean and sensitive to iron supply.

Following “the iron hypothesis” in the nineties (Martin 1990), iron limitation of high nutrient low chlorophyll (HNLC) areas, including the Southern Ocean, has been tested in bottle experiments (de Baar et al., 1990) and through *in situ* artificial fertilization experiments (de Baar et al., 2005; Boyd et al., 2007). Results from these experiments are numerous and essentially highlight that the lack of iron limits macronutrient (N, P, Si) utilization (Boyd et al., 2005; Hiscock and Millero, 2005) and primary production (Landry et al., 2000; Gall et al., 2001; Coale et al., 2004) in these vast HNLC areas of the Southern Ocean. Due to a large macronutrient repository the biological carbon pump in the Southern Ocean is considered to

be inefficient in its capacity to transfer atmospheric carbon to the ocean interior (Sarmiento and Gruber, 2006). In the context of micronutrient limitation, sites enriched in iron by natural processes have also been studied and include the Kerguelen islands (Blain et al., 2001, 2007), the Crozet islands (Pollard et al., 2007), the Scotia Sea (Tarling et al., 2012), and the Drake Passage (Measures et al., 2013). Enhanced primary producer biomass in association with natural iron supply (Korb and Whitehouse, 2004; Seeyave et al., 2007; Lefèvre et al., 2008) strongly support trace-metal limitation. Furthermore, indirect seasonal budgets constructed from studies of naturally fertilized systems have been capable of demonstrating an increase in the strength of the biological carbon pump (Blain et al., 2007; Pollard et al., 2009), although strong discrepancies in carbon to iron sequestration efficiency exist between systems. To date, direct measurements of POC export over seasonal cycles from naturally fertilized blooms in the Southern Ocean are limited to the Crozet Plateau (Pollard et al., 2009; Salter et al., 2012). The HNLC Southern Ocean represents a region where changes in the strength of the biological pump may have played a role in the glacial-interglacial CO_2 cycles (Bopp et al., 2003; Kohfeld et al., 2005) and have some significance to future anthropogenic CO_2 uptake (Sarmiento and Le Quéré, 1996). In this context, additional studies that directly measure POC export from naturally iron-fertilized blooms in the Southern Ocean are necessary.

POC export can be estimated at short timescales (days to weeks) using the ^{234}Th proxy (Coale and Bruland, 1985; Buesseler et al., 2006; Savoye et al., 2006), by optical imaging of particles (e.g. Picheral et al., 2010, Jouandet et al., 2011) or by directly collecting particles into surface-tethered sediment traps (e.g. Maiti et al., 2013 for a compilation in the Southern Ocean) or neutrally buoyant sediment traps (e.g. Salter et al., 2007; Rynearson et al., 2013). Temporal variability of flux in the Southern Ocean precludes extrapolation of discrete measurements to estimate seasonal or annual carbon export. However seasonal export of POC can be derived from biogeochemical budgets (Blain et al., 2007; Jouandet et al., 2011; Pollard

et al., 2009) or be directly measured by moored sediment traps (e.g. Salter et al., 2012). Biogeochemical budgets are capable of integrating over large spatial and temporal scales but may incorporate certain assumptions and lack information about underlying mechanisms. Direct measurement by sediment traps rely on fewer assumptions but their performance is strongly related to prevailing hydrodynamic conditions (Buesseler et al., 2007a), which can be particularly problematic in the surface ocean. Measuring the hydrological conditions characterizing mooring deployments is therefore crucial to address issues surrounding the efficiency of sediment trap collection.

The ecological processes responsible for carbon export remain poorly characterized (Boyd and Trull, 2007). There is a strong requirement for quantitative analysis of the biological components of export to elucidate patterns in carbon and biomineral fluxes to the ocean interior (Francois et al., 2002; Salter et al., 2010; Henson et al., 2012; Le Moigne et al., 2012; Lima et al., 2014). Long-term deployment of moored sediment traps in areas of naturally iron fertilized production, where significant macro- and micro-nutrient gradients seasonally structure plankton communities, can help to establish links between ecological succession and carbon export. For example, sediment traps around the Crozet Plateau (Pollard et al., 2009) identified the significance of *Eucampia antarctica* var. *antarctica* resting spores for carbon transfer to the deep ocean, large empty diatom frustules for Si:C export stoichiometry (Salter et al., 2012), and heterotrophic calcifiers for the carbonate counter pump (Salter et al., 2014).

The increase in primary production resulting from natural fertilization might not necessarily lead to significant increases in carbon export. The concept of "High Biomass, Low Export" (HBLE) environments was first introduced in the Southern Ocean (Lam and Bishop, 2007). This concept is partly based on the idea that a strong grazer response to phytoplankton biomass leads to major fragmentation and remineralization of particles in the twilight zone,

shallowing the remineralization horizon (Coale et al., 2004). In these environments, the efficient utilization and reprocessing of exported carbon by zooplankton leads to fecal pellet dominated, low POC fluxes (Ebersbach et al., 2011). A synthesis of short-term sediment trap deployments, ^{234}Th estimates of upper ocean POC export and in situ primary production measurements in the Southern Ocean by Maiti et al. (2013) has highlighted the inverse relationship between primary production and export efficiency, verifying the HBLE status of many productive areas in the Southern Ocean. The iron fertilized bloom above the Kerguelen Plateau exhibits strong remineralization in the mixed layer compared to the mesopelagic, (Jacquet et al., 2008) and high bacterial carbon demand (Obernosterer et al., 2008), features consistent with a HBLE regime. Moreover, an inverse relationship between export efficiency and zooplankton biomass in the Kerguelen Plateau region support the key role of grazers in the HBLE scenario (Laurenceau-Cornec et al., 2015). Efficient grazer responses to phytoplankton biomass following artificial iron fertilization of HNLC regions also demonstrate increases in net community production that are not translated to an increase in export fluxes (Lam and Bishop, 2007; Tsuda et al., 2007; Martin et al., 2013; Batten and Gower, 2014).

POC flux attenuation with depth results from processes occurring in the euphotic layer (setting the particle export efficiency, Henson et al., 2012) and processes occurring in the twilight zone between the euphotic layer and ~1000 m (Buesseler and Boyd, 2009), setting the transfer efficiency (Francois et al., 2002). These processes are mainly biologically-driven (Boyd and Trull, 2007) and involve a large diversity of ecosystem components from bacteria (Rivkin and Legendre, 2001; Giering et al., 2014), protozooplankton (Barbeau et al., 1996), mesozooplankton (Dilling and Alldredge, 2000; Smetacek et al., 2004) and mesopelagic fishes (Davison et al., 2013; Hudson et al., 2014). The net effect of these processes is summarized in a power-law formulation of POC flux attenuation with depth proposed by

Martin et al. (1987) that is still commonly used in data and model applications. The b-exponent in this formulation has been reported to range from 0.4 to 1.7 (Buesseler et al., 2007b; Lampitt et al., 2008; Henson et al., 2012) in the global ocean. Nevertheless, a change in the upper mesopelagic community structure (Lam et al., 2011), and more precisely an increasing contribution of mesozooplankton (Lam and Bishop, 2007; Ebersbach et al., 2011) could lead to a shift toward higher POC flux attenuation with depth.

In this paper, we provide the first annual description of the POC and PON export fluxes below the mixed layer within the naturally fertilized bloom of the Kerguelen Plateau and we discuss the reliability of these measurements considering the hydrological and biological context. A companion paper (Rembauville et al., 2014) addresses our final aim: to identify the ecological vectors that explain the intensity and the stoichiometry of the fluxes.

2 Material and Methods

2.1 Trap deployment and mooring design

As part of the KEOPS2 multidisciplinary program, a mooring line was deployed at station A3 (50°38.3 S – 72°02.6 E) in the Permanently Open Ocean Zone (POOZ), south of the Polar Front (PF) (Fig. 1). The mooring line was instrumented with a Technicap PPS3 (0.125 m^2 collecting area, 4.75 aspect ratio) sediment trap and inclinometer (NKE S2IP) at a depth of 289 m (seafloor depth 527 m) (Fig. 2). A conductivity-temperature-pressure (CTD) sensor (Seabird SBE 37) and a current meter (Nortek Aquadopp) were placed on the mooring line 30 m beneath the sediment trap (319 m). The sediment trap collection period started on 21 October 2011 until 7 September 2012. The sediment trap was composed of twelve rotating sample cups (250 mL) filled with a 5 % formalin hypersaline solution buffered with sodium tetraborate at pH = 8. Rotation of the carousel was programmed to sample short intervals (10-14 days) between October and February, to optimize the temporal resolution of export from the bloom, and long intervals (99 days) between February and September. All instruments had a 1 hour recording interval. The current meter failed on the 7th April 2012.

2.3 Surface chlorophyll data

The MODIS AQUA level 3 (4 km grid resolution, 8 day averages) surface chlorophyll *a* product was extracted from the NASA website (http://oceancolor.gsfc.nasa.gov/) for the sediment trap deployment period. An annual climatology of surface chlorophyll *a* concentration, based on available satellite products (1997-2013), was calculated from the multisatellite Globcolour product. The Globcolour level 3, (case 1 waters, 4.63 km resolution, 8 day averages) product merging Seawifs, MODIS and MERIS data with GSM merging model (Maritorena and Siegel, 2005) was accessed via http://www.globcolour.info. Surface chlorophyll *a* concentrations derived from Globcolour (climatology) and MODIS data

174 (deployment year) were averaged across a 100 km radius centered on the sediment trap
175 deployment location (Fig. 1).

176 **2.3 Time series analyses of hydrological parameters**

177 Fast Fourier Transform (FFT) analysis was performed on the annual time series data obtained
178 from the mooring, depth and potential density anomaly (σ_θ) that were derived from the CTD
179 sensor. Significant peaks in the power spectrum were identified by comparison to red noise, a
180 theoretical signal in which the relative variance decreases with increasing frequency (Gilman
181 et al., 1963). The red noise signal was considered as a null hypothesis and its power spectrum
182 was scaled to the 99^{th} percentile of χ^2 probability. Power peaks higher than 99 % red noise
183 values were considered to be statistically significant (Schulz and Mudelsee, 2002), enabling
184 the identification of periods of major variability in time series. In order to identify the water
185 masses surrounding the trap, temperature and salinity recorded by the mooring CTD were
186 placed in context to previous CTD casts conducted at A3 during KEOPS1 (39 profiles, 23
187 January 2005 - 13 February 2005) and KEOPS2 (12 profiles, from 15 - 17 November).

188 **2.4 Sediment trap material analyses**

189 Upon recovery of the sediment trap the pH of the supernatant was measured in every cup and
190 1 mL of 37 % formalin buffered with sodium tetraborate (pH=8) was added. After allowing
191 the particulate material to settle to the base of the sample cup (~24 hrs), 60 mL of supernatant
192 was removed with a syringe and stored separately. The samples were transported in the dark
193 at 4°C (JGOFS Sediment Trap Methods, 1994) and stored under identical conditions upon
194 arrival at the laboratory until further analysis. Nitrate, nitrite, ammonium and phosphate in the
195 supernatant were analysed colorimetrically (Aminot and Kerouel, 2007) to check for possible
196 leaching of dissolved inorganic nitrogen and phosphorus from the particulate phase.

Samples were first transferred to a petri dish and examined under stereomicroscope (Leica MZ8, x10 to x50 magnification) to determine and isolate swimmers (i.e. organisms that actively entered the cup). All swimmers were carefully sorted, cleaned (rinsed with preservative solution), enumerated and removed from the cups for further taxonomic identification. The classification of organisms as swimmers remains subjective and there is no standardized protocol. We classified zooplankton organisms as swimmers if organic material and preserved structures could be observed. Empty shells, exuvia (exoskeleton remains) and organic debris were considered part of the passive flux. Sample preservation prevented the identification of smaller swimmers (mainly copepods) but, where possible, zooplankton were identified following Boltovskoy (1999).

Following the removal of swimmers, samples were quantitatively split into eight aliquots using a Jencons peristaltic splitter. A splitting precision of 2.9 % (coefficient of variation) was determined by weighing the particulate material obtained from each of four $1/8^{th}$ aliquots (see below). Aliquots for chemical analyses were centrifuged (5 min at 3000 rpm) with the supernatant being withdrawn after this step and replaced by Milli-Q-grade water to remove salts. Milli-Q rinses were compared with ammonium formate. Organic carbon content was not statistically different although nitrogen concentrations were significantly higher, consequently Milli-Q rinses were routinely performed. The rinsing step was repeated three times. The remaining pellet was freeze-dried (SGD-SERAIL, 0.05-0.1 mbar, -30 °C to 30 °C, 48h run) and weighed three times (Sartorius MC 210 P balance, precision 10^{-4} g) to calculate the total mass. The particulate material was ground to a fine powder and used for measurements of particulate constituents.

For particulate organic carbon (POC) and particulate organic nitrogen (PON) analyses, 3 to 5 mg of the freeze-dried powder was weighed directly into pre-combusted (450°C, 24h) silver cups. Samples were decarbonated by adding 20 µL of 2M analytical grade hydrochloric

222 acid (Sigma-Aldrich). Acidification was repeated until no bubbles could be seen, ensuring all
223 particulate carbonate was dissolved (Salter et al., 2010). Samples were dried overnight at 50
224 °C. POC and PON were measured with a CHN analyzer (Perkin Elmer 2400 Series II
225 CHNS/O Elemental Analyzer) calibrated with glycine. Samples were analysed in triplicate
226 with an analytical precision of less than 0.7 %. Due to the small amount of particulate
227 material in sample cups #5 and #12, replicate analyses were not possible. Uncertainty
228 propagation for POC and PON flux was calculated as the quadratic sum of errors on mass flux
229 and POC/PON content in each sample. The annual flux (± standard deviation) was calculated
230 as the sum of the time-integrated flux.

231 **3. Results**

232 **3.1 Physical conditions around trap**

233 The sediment trap was deployed in the upper layers of Upper Circumpolar Deep Water
234 (UCDW), beneath seasonally mixed Winter Water (WW) (Fig. 2). The depth of the CTD
235 sensor varied between 318 m and 322 m (1 % and 99 % quantiles), with rare deepening to 328
236 m (Fig. 3a). Variations in tilt angle of the sediment trap were also low, mostly between 1 °
237 and 5 °, and occasionally reaching 13 ° (Fig. 3d). Current speed amplitude varied between 4
238 cm s^{-1} and 23 cm s^{-1} (1 % and 99 % quantiles) with a maximum value of 33 cm s^{-1} and a mean
239 value of 9 cm s^{-1} (Fig. 3e). Horizontal flow vectors were divided between northward and
240 southward components with strongest current speeds observed to flow northward (Fig. 3f and
241 3g).

242 The range in potential temperature and salinity was 1.85–2.23 °C and 34.12 – 34.26 (1
243 % - 99 % quantiles) (Fig. 3b and 3c). From July to September 2012, a mean increase of 0.2°C
244 in potential temperature was associated with a strong diminution of high frequency noise
245 suggesting a drift of the temperature sensor. Consequently these temperature data were

246 rejected from the time-series analysis. The potential temperature/salinity diagram is compared
247 to KEOPS1 and KEOPS2 CTD downcast at station A3 (Fig. 4). The CTD sensor recorded the
248 signature of the UCDW and no intrusion of overlying WW could be detected.

249 The power spectrum of vertical sediment trap displacements identified six significant
250 peaks corresponding to frequencies of 6.2 h, 8.2 h, 23.9 h, 25.7 h and 14 days (Fig 5a).
251 Concomitant peaks of depth, angle and current speed were also observed with a period of 14
252 days. However, spectral analysis of the potential density anomaly σ_θ revealed only one
253 significant major power peak corresponding to a frequency of 12.4 h (Fig. 5b). Isopycnal
254 displacements were driven by the unique tidal component (M2, 12.4h period) and trap
255 displacements resulted from a complex combination of multiple tidal components. The power
256 spectrum analysis suggested that a 40 hour window was relevant to filter out most of the short
257 term variability (black line in Fig 3a – 3e).

258 A pseudo-lagrangian trajectory was calculated by cumulating the instantaneous current
259 vectors (Fig 6). Over short time-scales (hours to day) the trajectory displays numerous tidal
260 ellipses. The flow direction is mainly to the South-East in October 2011 to December 2012
261 and North-East from December 2011 to April 2012. For the entire current meter record (6
262 months) the overall displacement followed a 120 km northeasterly, anticlockwise trajectory
263 with an effective eastward current speed of approximately 1 cm s^{-1}.

264 **3.2 Seasonality of surface chlorophyll *a* concentration above trap location**

265 The seasonal variations of surface chlorophyll *a* concentration for the sediment trap
266 deployment period differed significantly from the long-term climatology (Fig 7a). The bloom
267 started at the beginning of November 2011, ten days after the start of the sediment trap
268 deployment. Maximum surface chlorophyll *a* values of 2.5 µg L^{-1} occurred on the first week
269 of November and subsequently declined rapidly to 0.2 µg L^{-1} in late December 2011. A

second increase in surface chlorophyll *a* up to 1 µg L^{-1} occurred in January 2012 and values decreased to winter levels of 0.2 µg L^{-1} in February 2012. A short-term increase of 0.8 µg L^{-1} occurred in mid-April 2012.

3.3 Swimmer abundances

No swimmers were found in cups #3 and #5 (Table 2). Total swimmer numbers were highest in winter (1544 individuals in cup #12). When normalized to cup opening time, swimmer intrusion rates were highest between mid-December 2011 and mid-February 2012 (from 26 to 55 individuals d^{-1}) and lower than 20 individuals d^{-1} for the remainder of the year. Swimmers were numerically dominated by copepods throughout the year, but elevated amphipod and pteropod abundances were observed at the end of January and February 2012 (Table 2). There was no significant correlation between mass flux, POC and PON fluxes and total swimmer number or intrusion rate (Spearman's correlation test, p >0.01). Copepods were essentially small cyclopoid species. Amphipods were predominantly represented by the hyperidean *Cyllopus magellanicus* and *Themisto gaudichaudii*. Pteropods were represented by *Clio pyramidata*, *Limacina helicina* forma *antarctica* and *Limacina retroversa* subsp. *australis*. Euphausiids were only represented by the genus *Thysanoessa*. One *Slapa thompsoni* salp (aggregate form) was found in the last winter cup #12.

3.4 Seasonal particulate organic carbon and nitrogen fluxes

Particulate organic carbon flux ranged from 0.15 to 0.55 mmol m^{-2} d^{-1} during the productive period except during two short export events of 1.6 ± 0.04 and 1.5 ± 0.04 mmol m^{-2} d^{-1} sampled in cups #4 (2 to 12 December 2011) and #9 (25 January to 8 February 2012), respectively (Fig. 7b). The two flux events occurred with an approximate time lag of one month compared to peaks in surface chlorophyll *a* values. A modest value of 0.27±0.01 mmol m^{-2} d^{-1} was observed in autumn (cup #11, 22 February to 30 May 2012). The lowest POC flux

was measured during winter (0.04 mmol m^{-2} d^{-1}, cup #12, 31 May to 7 October). Assuming that POC export was negligible from mid September to mid October, the annually integrated POC flux was 98.2 ± 4.4 mmol m^{-2} y^{-1} (Table 1). The two short (<14 days) export events accounted for 16.2±0.5 % (cup #4) and 21.0±0.6 % (cup #9) of the annual carbon export out of the mixed layer (Table 1). Mass percentage of organic carbon ranged from 3.3 % to 17.4 % (Fig. 7b). Values were slightly higher in autumn and winter (respectively 13.1±0.2 % and 11±2.1 % in cups #11 and #12) than in the summer, with the exception of cup #5 where the highest value of 17.4 % was observed. PON fluxes followed the same seasonal patterns as POC. This resulted in a relatively stable POC:PON ratio that varied between 6.1 to 7.4, except in the autumn cup #11 where it exceeded 8.1 (Table 1).

4 Discussion

4.1 Physical conditions of trap deployment

Moored sediment traps can be subject to hydrodynamic biases that affect the accuracy of particle collection (Buesseler et al., 2007a). The aspect ratio, tilt and horizontal flow regimes are important considerations when assessing sediment trap performance. Specifically, the line angle and aspect ratio of cylindrical traps can result in oversampling (Hawley, 1988). Horizontal current velocities of 12 cm s^{-1} are often invoked as a critical threshold over which particles are no longer quantitatively sampled (Baker et al., 1988). During the sediment trap deployment period we observed generally low current speeds (mean < 10 cm s^{-1}) with 75% of the recorded data lower than 12 cm s^{-1}. Despite the high aspect ratio of the PPS3 trap (4.75), and the small mooring line angle deviations, it is likely that episodic increases in current velocities (>12 cm s^{-1}) impacted collection efficiency. When integrated over the entire current meter record (October 2011 to April 2012), the resulting flow is consistent with the annual

northeastward, low velocity (~ 1 cm s^{-1}) geostrophic flow previously reported over the central part of the Kerguelen plateau (Park et al., 2008b).

The depth of the winter mixed layer (WML) on the Kerguelen Plateau is usually shallower than 250 m (Park et al., 1998; Metzl et al., 2006). The sediment trap deployment depth of ~300 m was selected to sample particle flux exiting the WML. The moored CTD sensor did not record any evidence of a winter water incursion during the deployment period, confirming the WML did not reach the trap depth. The small depth variations observed during the deployment period resulted from vertical displacement of the trap. Variations of σ_θ may have resulted from both vertical displacement of the CTD sensor and possible isopycnal displacements due to strong internal waves that can occur with an amplitude of > 50 m at this depth (Park et al., 2008a). Our measurements demonstrate that isopycnal displacements are consistent with the M2 (moon 2, 12.4 h period) tidal forcing described in physical modeling studies (Maraldi et al., 2009, 2011). Spectral analysis indicates that high frequency tidal currents are the major circulation components. Time-integrated currents suggest that advection is weak and occurs over longer timescale (months). Assuming the current flow measured at the sediment trap deployment depth is representative of the prevailing current under the WML, more than three months are required for particles to leave the plateau from the A3 station, a timescale larger than the bloom duration itself. Therefore we consider that the particles collected in the sediment trap at station A3 were produced in the surface waters located above the plateau during bloom conditions.

4.2 Swimmers and particle solubilization

Aside from the hydrodynamic effects discussed above, other potential biases characterizing sediment trap deployments, particularly those in shallow waters, is the presence of swimmers and particle solubilization. Swimmers can artificially increase POC fluxes by entering the

cups and releasing particulate organic matter or decrease the flux by feeding in the trap funnel (Buesseler et al., 2007a). Some studies have focused specifically on swimmer communities collected in shallow sediment traps (Matsuno et al., 2014 and references therein) although trap collection of swimmers is probably selective and therefore not quantitative. Total swimmer intrusion rate was highest in cups #6 to #9 (December 2011 to February 2012) generally through the representation of copepods and amphipods (Table 2). The maximum swimmer intrusion rate in mid-summer as well as the copepod dominance is consistent with the fourfold increase in mesozooplankton abundance observed from winter to summer (Carlotti et al., 2014). Swimmer abundance was not correlated with mass flux, POC or PON fluxes, suggesting that their presence did not systematically affect particulate fluxes inside the cups. Nevertheless such correlations cannot rule out the possibility of swimmers feeding in the trap funnel modifying particle flux collection.

Particle solubilization in preservative solutions may also lead to an underestimation of total flux measured in sediment traps. Previous analyses from traps poisoned with mercuric chloride suggest that ~30 % of total organic carbon flux can be found in the dissolved phase and much higher values of 50 % and 90 % may be observed for nitrogen and phosphorous, respectively (Antia, 2005; O'Neill et al., 2005). Unfortunately the use of a formaldehyde-based preservative in our trap samples precludes any direct estimate of excess of dissolved organic carbon in the sample cup supernatant. Furthermore, corrections for particle leaching have been considered problematic in the presence of swimmers since a fraction of the leaching may originate from the swimmers themselves (Antia, 2005), potentially leading to over-correction. Particles solubilization may have occurred in our samples as evidenced by excess PO_4^{3-} in the supernatant. However the largest values were measured in sample cups where total swimmers were abundant (cups #8 to #12, data not shown). Consequently, it was not possible to discriminate solubilisation of P from swimmers and passively settling particles

366 and it therefore remains difficult to quantify the effect of particle leaching. However, leaching
367 of POC should be less problematic in formalin-preserved samples because aldehydes fix
368 organic matter, in addition to poisoning microbial activity.

369 **4.3 Seasonal dynamics of POC export**

370 The sediment trap record obtained from station A3 provides the first direct estimate of POC
371 export covering an entire season over the naturally fertilized Kerguelen Plateau. We observed
372 a temporal lag of one month between the two surface chlorophyll *a* peaks and the two export
373 events. Based on a compilation of annual sediment trap deployments, Lutz et al. (2007)
374 reported that export quickly follows primary production at low latitudes whereas a time lag up
375 to two months could occur at higher latitudes. A 1-2 month lag was observed between
376 production and export in the pacific sector of the Southern Ocean (Buesseler et al., 2001), as
377 well as along 170°W (Honjo et al., 2000) and in the Australian sector of the Subantarctic
378 Zone (Rigual-Hernández et al., 2015). The temporal lag between surface production and
379 measured export in deep traps can originate from ecological processes in the upper ocean (e.g.
380 carbon retention in the mixed layer) as well as slow sinking velocities (Armstrong et al.,
381 2009) and one cannot differentiate the two processes from a single deep trap signal. A global-
382 scale modeling study suggests that the strongest temporal decoupling between production and
383 export (more than one month) occurs in areas characterized by a strong seasonal variability in
384 primary production (Henson et al., 2014). The study attributes this decoupling to differences
385 in phenology of phytoplankton and zooplankton and evokes zooplankton ejection products as
386 major contributors to fast sinking particles sedimenting post bloom.

387 On the Kerguelen Plateau there is evidence that a significant fraction of
388 phytoplankton biomass comprising the two chlorophyll peaks is remineralized by a highly
389 active heterotrophic microbial community (Obernosterer et al., 2008; Christaki et al., 2014).
390 Another fraction is likely channeled toward higher trophic levels through the intense grazing

391 pressure that supports the observed increase in zooplankton biomass (Carlotti et al., 2008,
392 2014). Therefore an important fraction of phytoplankton biomass increases observed by
393 satellite may not contribute to export fluxes. Notably, the POC:PON ratio measured in our
394 trap material is close to values reported for marine diatoms (7.3 ± 1.2, Sarthou et al., 2005),
395 compared to the C:N ratio of zooplankton faecal pellets which is typically higher (7.3 to >15,
396 Gerber and Gerber, 1979; Checkley and Entzeroth, 1985; Morales, 1987). Simple mass
397 balance would therefore suggest a significant contribution of phytoplanktonic cells to the
398 POC export, which is indeed corroborated by detailed microscopic analysis (Rembauville et
399 al., 2014).

400 Although we observed increasing contributions of faecal pellet carbon post-bloom
401 (Rembauville et al., 2014), in line with the model output of Henson et al. (2014), differences
402 in phytoplankton and zooplankton phenology do not fully explain the seasonality of export on
403 the Kerguelen Plateau. Considering the shallow trap depth (289 m) and typical sinking speed
404 of 100 m d^{-1} for phyto-aggregates (Allredge and Gotschalk, 1988; Peterson et al., 2005; Trull
405 et al., 2008a), aggregate-driven export following bloom demise would suggest a short lag of a
406 few days between production and export peaks. The temporal lag of one month measured in
407 the present study suggest either slow sinking rates (<5 m d^{-1}) characteristic of single
408 phytoplanktonic cells or faster sinking particles that originate from sub-surface production
409 peaks undetected by satellite. It is generally accepted that satellite detection depth is 20-50 m
410 (Gordon and McCluney, 1975), and can be less than 20 m when surface chlorophyll *a* exceed
411 0.2 µg L^{-1} (Smith, 1981), which prevents the detection of deep phytoplanktonic biomass
412 structures (Villareal et al., 2011). Although subsurface chlorophyll maxima located around
413 100 m have been observed over the Kerguelen Plateau at the end of the productive period,
414 they have been interpreted to result from the accumulation of surface production at the base of
415 the mixed layer rather than subsurface productivity features (Uitz et al., 2009). In support of

this, detailed taxonomic analysis of the exported material highlights diatom resting spores as major contributors to the two export fluxes rather than a composite surface community accumulated at the base of the mixed layer. The hypothesis of a mass production of nutrient-limited resting spores post-bloom with high settling rates explains the temporal patterns of export we observed (Rembauville et al., 2014). However a better knowledge of the dynamics of factors responsible for resting spore formation by diatoms remains necessary to fully validate this hypothesis.

4.4 Evidence for significant flux attenuation over the Kerguelen Plateau

The Kerguelen Plateau annual POC export (98.2±4.4 mmol m^{-2} y^{-1}) approaches the median global ocean POC export value comprising shallow and deep sediment traps (83 mmol m^{-2} y^{-1}, Lampitt and Antia, 1997), but is also close to values observed in HNLC areas of the POOZ (11-43 mmol m^{-2} y^{-1} at 500 m, Fischer et al., 2000). Moreover, the magnitude of annual POC export measured at ~300m on the Kerguelen Plateau is comparable to deep-ocean (>2 km) POC fluxes measured from the iron-fertilized Crozet (60 mmol m^{-2} y^{-1},Salter et al., 2012) and South Georgia blooms (180 mmol m^{-2} y^{-1}, Manno et al., 2014).

We first compared the sediment trap export fluxes with short-term estimates at 200 m in spring (KEOPS2) and summer (KEOPS1). The POC flux recorded in the moored sediment trap represents only a small fraction (3-8%) of the POC flux measured at the base of the winter mixed layer (200 m) by different approaches during the spring KEOPS2 cruise (Table 3). The same conclusion can be drawn when considering the comparison with different estimates made at the end of summer during KEOPS1. Moreover, the annual POC export of ~0.1 mol m^{-2} y^{-1} at 289 m (Table 1) represents only 2% of the indirect estimate of POC export (5.1 mol m^{-2} y^{-1}) at the base of the WML (200 m) on the Kerguelen Plateau based on a seasonal DIC budget (Blain et al., 2007). The short term estimates are derived from a diverse range of methods. The ^{234}Th proxy is based on the ^{234}Th deficit relative to the ^{238}U due to its

441 adsorption on particles, and it subsequent conversion to carbon fluxes using measured
442 POC:^{234}Th ratios. (Coale and Bruland, 1985; Buesseler et al., 2006; Savoye et al., 2006). The
443 UVP (Underwater Video Profiler) provides high resolution images of particles (>52 µm) and
444 the particle size distribution is then converted to carbon fluxes using an empirical relationship
445 (Guidi et al., 2008; Picheral et al., 2010). Drifting gel traps allows the collection, preservation
446 and imaging of sinking particles (>71 µm) that are converted to carbon fluxes using empirical
447 volume:carbon relationship (Ebersbach and Trull, 2008; Ebersbach et al., 2011; Laurenceau-
448 Cornec et al., 2015). Finally, drifting sediment traps are conceptually similar to moored
449 sediment traps but avoid most of the hydrodynamic biases associated with this technique
450 (Buesseler et al., 2007a). The diversity of the methods and differences in depth where the
451 POC flux was estimated render quantitative comparisons challenging. Nevertheless, POC
452 fluxes measured at 289 m with the moored sediment trap are considerably lower than other
453 estimates made at 200 m. This result indicates either extremely rapid attenuation of flux
454 between 200 m and 300 m or significant sampling bias by the sediment trap.

455 We note that low carbon export fluxes around 300 m have been previously reported on
456 the Kerguelen Plateau. In spring 2011, UVP derived estimates of POC export at 350 m were
457 0.1 to 0.3 mmol m^{-2} d^{-1} (Table 3), values close to our reported value of 0.15 mmol m^{-2} d^{-1}. In
458 summer 2005, POC export at 330 m from gel trap was 0.7 mmol m^{-2} d^{-1} (Ebersbach and Trull
459 2008), which is also close to our value of 1.5 mmol m^{-2} d^{-1}. Using the Jouandet et al. (2014)
460 data at 200 m (1.9 mmol m^{-2} d^{-1}) and 350 m (0.3 mmol m^{-2} d^{-1}) and the Ebersbach and Trull
461 (2008) data at 200 m (5.2 mmol m^{-2} d^{-1}) and 330 m (0.7 mmol m^{-2} d^{-1}) leads to Martin power
462 law exponents values of 3.3 and 4, respectively. These values are high when compared to the
463 range of 0.4–1.7 that was initially compiled for the global ocean (Buesseler et al., 2007b).
464 However, there is increasing evidence in support of much higher b-values in the Southern
465 Ocean that fall in the range 0.9-3.9 (Lam and Bishop, 2007; Henson et al., 2012; Cavan et al.,

466 2015). Our calculations are thus consistent with emerging observations of significant POC
467 flux attenuation in the Southern Ocean.

468 Using the aforementioned b values (3.3 and 4) and the POC flux derived from ^{234}Th
469 deficit at 200 m in spring (Planchon et al., 2014), we estimate POC fluxes at 289 m of 0.7 to
470 1.1 mmol m^{-2} d^{-1}. The flux measured in our sediment trap (0.15 mmol m^{-2} d^{-1}) data represents
471 14 % to 21 % of this calculated flux. Very similar percentages (21 % to 27 %) are found using
472 the POC fluxes derived from the ^{234}Th deficit in summer (Savoye et al., 2008). Therefore we
473 consider that the moored sediment trap collected ~15-30 % of the ^{234}Th – derived particle flux
474 equivalent throughout the year. Trap-derived particle fluxes can represent 0.1 to >3 times the
475 ^{234}Th-derived particles in shallow sediment traps (Buesseler, 1991; Buesseler et al., 1994;
476 Coppola et al., 2002; Gustafsson et al., 2004) and this difference is largely attributed to the
477 sum of hydrodynamic biases and swimmer activities (Buesseler, 1991), although it probably
478 also includes the effect of post-collection particle solubilisation. In the Antarctic Peninsula,
479 ^{234}Th derived POC export was 20 times higher than the fluxes collected by a shallow,
480 cylindrical, moored sediment trap at 170 m (Buesseler et al., 2010). The present deployment
481 context is less extreme (depth of 289 m, mean current speed <10 cm s^{-1}, low tilt angle, high
482 aspect ratio of the cylindrical PPS3 trap) but we consider that hydrodynamics (current speed
483 higher than 12 cm s^{-1} during short tidal-driven events) and possible zooplankton feeding on
484 the trap funnel are potential biases that may explain in part the low fluxes recorded by the
485 moored sediment trap. Therefore the low fluxes observed likely result from a combined effect
486 of collection bias (hydrodynamics and swimmers) and attenuation of the POC flux between
487 the base of the WML and 300 m. However, it is not possible with the current dataset to isolate
488 a specific explanation for low flux values.

489 Strong POC flux attenuation over the Kerguelen Plateau compared to the open ocean
490 is also reported by Laurenceau-Cornec et al. (2015) who associated this characteristic with a

HBLE scenario and invoked the role of mesozooplankton in the carbon flux attenuation. Between October and November 2011, mesozooplankton biomass in the mixed layer doubled (Carlotti et al., 2014) and summer biomass was twofold higher still (Carlotti et al., 2008). These seasonal patterns are consistent with the maximum swimmer intrusion rate and swimmer diversity observed in summer (Table 2). It has previously been concluded that zooplankton biomass is more tightly coupled to phytoplankton biomass on the plateau compared to oceanic waters, leading to higher secondary production on the plateau (Carlotti et al., 2008, 2014). Further support linking zooplankton dynamics to HBLE environments of iron-fertilized blooms are the findings of Cavan et al. (2015) that documents the lowest export ratio (exported production/primary production) in the most productive, naturally fertilized area downstream of South Georgia. Another important ecosystem feature associated to the HBLE environment of the Kerguelen Plateau, and likely shared by other island-fertilized blooms in the Southern Ocean, is the presence of mesopelagic fish (myctophid spawning and larvae foraging site, Koubbi et al., 1991, 2001). Mesopelagic fish can be tightly coupled to lower trophic levels (Saba and Steinberg, 2012) and can play a significant role in carbon flux attenuation (Davison et al., 2013). Although important for carbon budgets it is a compartment often neglected due to the challenge of quantitative sampling approaches. We suggest that the HBLE scenario and large attenuation of carbon flux beneath the WML at Kerguelen may reflect the transfer of carbon biomass to higher and mobile trophic groups that fuel large mammal and bird populations rather than the classical remineralization-controlled attenuation characterizing open ocean environments. Although technically challenging, testing this hypothesis should be a focus for future studies in this and similar regions.

5. Conclusion

We report the seasonal dynamics of particulate organic carbon (POC) export under the winter mixed layer (289 m) of the naturally iron fertilized and productive central Kerguelen Plateau.

Annual POC flux was remarkably low (98 mmol m^{-2}) and occurred primarily during two episodic (<14 days) flux events exported with a 1 month lag following two surface chlorophyll *a* peaks. Analysis of the hydrological conditions and a comparison with different estimates of POC fluxes in spring and summer at the same station suggests that the sediment trap was subject to possible hydrodynamic and biological biases leading to under collection of particle flux. Nevertheless the low POC export was close to other estimates of deep (>300 m) POC export at the same station and is consistent with high attenuation coefficients reported from other methods. We invoke heterotrophic microbial activity and mesozooplankton and mesopelagic fish activity as possible explanations for efficient carbon flux attenuation and/or transfer to higher trophic levels which results in a High Biomass, Low Export environment.

The biogenic silicon, diatoms assemblages and faecal pellet fluxes are reported in a companion paper that identifies the primary ecological vectors regulating the magnitude of POC export and seasonal patterns in BSi:POC export (Rembauville et al., 2014).

Acknowledgements

We thank the Chief Scientist Prof. Bernard Quéguiner, the Captain Bernard Lassiette and his crew during the KEOPS2 mission on the R/V Marion Dufresne II. We thank Leanne Armand and Tom Trull for their constructive comments, as well as three anonymous reviewers which helped us to improve the manuscript. This work was supported by the French Research program of INSU-CNRS LEFE-CYBER (Les enveloppes fluides et l'environnement – Cycles biogéochimiques, environnement et ressources), the French ANR (Agence Nationale de la Recherche, SIMI-6 program, ANR-10-BLAN-0614), the French CNES (Centre National d'Etudes Spatiales) and the French Polar Institute IPEV (Institut Polaire Paul-Emile Victor).

References

Allredge, A.L., Gotschalk, C., 1988. In situ settling behavior of marine snow. Limnol. Oceanogr. 33, 339–351.

Aminot, A., Kerouel, R., 2007. Dosage automatique des nutriments dans les eaux marines: méthodes en flux continu. Ifremer, Plouzané, France.

Antia, A.N., 2005. Solubilization of particles in sediment traps: revising the stoichiometry of mixed layer export. Biogeosciences 2, 189–204. doi:10.5194/bg-2-189-2005

Armstrong, R.A., Peterson, M.L., Lee, C., Wakeham, S.G., 2009. Settling velocity spectra and the ballast ratio hypothesis. Deep Sea Res. Part II Top. Stud. Oceanogr. 56, 1470–1478. doi:10.1016/j.dsr2.2008.11.032

Arrigo, K.R., Worthen, D., Schnell, A., Lizotte, M.P., 1998. Primary production in Southern Ocean waters. J. Geophys. Res. Oceans 103, 15587–15600. doi:10.1029/98JC00930

Baker, E.T., Milburn, H.B., Tennant, D.A., 1988. Field assessment of sediment trap efficiency under varying flow conditions. J. Mar. Res. 46, 573–592. doi:10.1357/002224088785113522

Barbeau, K., Moffett, J.W., Caron, D.A., Croot, P.L., Erdner, D.L., 1996. Role of protozoan grazing in relieving iron limitation of phytoplankton. Nature 380, 61–64. doi:10.1038/380061a0

Batten, S.D., Gower, J.F.R., 2014. Did the iron fertilization near Haida Gwaii in 2012 affect the pelagic lower trophic level ecosystem? J. Plankton Res. 36, 925–932. doi:10.1093/plankt/fbu049

Blain, S., Quéguiner, B., Armand, L., Belviso, S., Bombled, B., Bopp, L., Bowie, A., Brunet, C., Brussaard, C., Carlotti, F., Christaki, U., Corbière, A., Durand, I., Ebersbach, F., Fuda, J.-L., Garcia, N., Gerringa, L., Griffiths, B., Guigue, C., Guillerm, C., Jacquet, S., Jeandel, C., Laan, P., Lefèvre, D., Lo Monaco, C., Malits, A., Mosseri, J., Obernosterer, I., Park, Y.-H., Picheral, M., Pondaven, P., Remenyi, T., Sandroni, V., Sarthou, G., Savoye, N., Scouarnec, L., Souhaut, M., Thuiller, D., Timmermans, K., Trull, T., Uitz, J., van Beek, P., Veldhuis, M., Vincent, D., Viollier, E., Vong, L., Wagener, T., 2007. Effect of natural iron fertilization on carbon sequestration in the Southern Ocean. Nature 446, 1070–1074. doi:10.1038/nature05700

Blain, S., Tréguer, P., Belviso, S., Bucciarelli, E., Denis, M., Desabre, S., Fiala, M., Martin Jézéquel, V., Le Fèvre, J., Mayzaud, P., Marty, J.-C., Razouls, S., 2001. A biogeochemical study of the island mass effect in the context of the iron hypothesis: Kerguelen Islands, Southern Ocean. Deep Sea Res. Part Oceanogr. Res. Pap. 48, 163–187. doi:10.1016/S0967-0637(00)00047-9

Boltovskoy, D., 1999. South Atlantic zooplankton. Backhuys.

Bopp, L., Kohfeld, K.E., Le Quéré, C., Aumont, O., 2003. Dust impact on marine biota and atmospheric CO2 during glacial periods. Paleoceanography 18, 1046. doi:10.1029/2002PA000810

Boyd, P.W., Jickells, T., Law, C.S., Blain, S., Boyle, E.A., Buesseler, K.O., Coale, K.H., Cullen, J.J., Baar, H.J.W. de, Follows, M., Harvey, M., Lancelot, C., Levasseur, M., Owens, N.P.J., Pollard, R., Rivkin, R.B., Sarmiento, J., Schoemann, V., Smetacek, V., Takeda, S., Tsuda, A., Turner, S., Watson, A.J., 2007. Mesoscale Iron Enrichment Experiments 1993-2005: Synthesis and Future Directions. Science 315, 612–617. doi:10.1126/science.1131669

Boyd, P.W., Law, C.S., Hutchins, D.A., Abraham, E.R., Croot, P.L., Ellwood, M., Frew, R.D., Hadfield, M., Hall, J., Handy, S., Hare, C., Higgins, J., Hill, P., Hunter, K.A., LeBlanc, K., Maldonado, M.T., McKay, R.M., Mioni, C., Oliver, M., Pickmere, S., Pinkerton, M., Safi, K., Sander, S., Sanudo-Wilhelmy, S.A., Smith, M., Strzepek, R., Tovar-Sanchez, A., Wilhelm, S.W., 2005. FeCycle: Attempting an iron biogeochemical budget from a mesoscale SF6 tracer experiment in unperturbed low iron waters. Glob. Biogeochem. Cycles 19, GB4S20. doi:10.1029/2005GB002494

Boyd, P.W., Trull, T.W., 2007. Understanding the export of biogenic particles in oceanic waters: Is there consensus? Prog. Oceanogr. 72, 276–312. doi:10.1016/j.pocean.2006.10.007

Buesseler, K.O., 1991. Do upper-ocean sediment traps provide an accurate record of particle flux? Nature 353, 420–423. doi:10.1038/353420a0

Buesseler, K.O., Antia, A.N., Chen, M., Fowler, S.W., Gardner, W.D., Gustafsson, Ö., Harada, K., Michaels, A.F., Rutgers v. d. Loeff, M., Sarin, M., Steinberg, D.K., Trull, T., 2007a. An assessment of the use of sediment traps for estimating upper ocean particle fluxes. J. Mar. Res. 65, 345–416.

Buesseler, K.O., Ball, L., Andrews, J., Cochran, J.K., Hirschberg, D.J., Bacon, M.P., Fleer, A., Brzezinski, M., 2001. Upper ocean export of particulate organic carbon and biogenic silica in the Southern Ocean along 170°W. Deep Sea Res. Part II Top. Stud. Oceanogr. 48, 4275–4297. doi:10.1016/S0967-0645(01)00089-3

Buesseler, K.O., Benitez-Nelson, C.R., Moran, S.B., Burd, A., Charette, M., Cochran, J.K., Coppola, L., Fisher, N.S., Fowler, S.W., Gardner, W.D., Guo, L.D., Gustafsson, Ö., Lamborg, C., Masque, P., Miquel, J.C., Passow, U., Santschi, P.H., Savoye, N., Stewart, G., Trull, T., 2006. An assessment of particulate organic carbon to thorium-234 ratios in the ocean and their impact on the application of 234Th as a POC flux proxy. Mar. Chem., Future Applications of 234Th in Aquatic Ecosystems (FATE) 100, 213–233. doi:10.1016/j.marchem.2005.10.013

Buesseler, K.O., Boyd, P.W., 2009. Shedding light on processes that control particle export and flux attenuation in the twilight zone of the open ocean. Limnol. Oceanogr. 54, 1210–1232. doi:10.4319/lo.2009.54.4.1210

Buesseler, K.O., Lamborg, C.H., Boyd, P.W., Lam, P.J., Trull, T.W., Bidigare, R.R., Bishop, J.K.B., Casciotti, K.L., Dehairs, F., Elskens, M., Honda, M., Karl, D.M., Siegel, D.A., Silver, M.W., Steinberg, D.K., Valdes, J., Mooy, B.V., Wilson, S., 2007b. Revisiting Carbon Flux Through the Ocean's Twilight Zone. Science 316, 567–570. doi:10.1126/science.1137959

Buesseler, K.O., McDonnell, A.M.P., Schofield, O.M.E., Steinberg, D.K., Ducklow, H.W., 2010. High particle export over the continental shelf of the west Antarctic Peninsula. Geophys. Res. Lett. 37, L22606. doi:10.1029/2010GL045448

Buesseler, K.O., Michaels, A.F., Siegel, D.A., Knap, A.H., 1994. A three dimensional time-dependent approach to calibrating sediment trap fluxes. Glob. Biogeochem. Cycles 8, 179–193. doi:10.1029/94GB00207

Carlotti, F., Thibault-Botha, D., Nowaczyk, A., Lefèvre, D., 2008. Zooplankton community structure, biomass and role in carbon fluxes during the second half of a phytoplankton bloom in the eastern sector of the Kerguelen Shelf (January–February 2005). Deep Sea Res. Part II Top. Stud. Oceanogr. 55, 720–733. doi:10.1016/j.dsr2.2007.12.010

Cavan, E.L., Le Moigne, F. a. c., Poulton, A.J., Tarling, G.A., Ward, P., Daniels, C.J., Fragoso, G., Sanders, R.J., 2015. Zooplankton fecal pellets control the attenuation of particulate organic carbon flux in the Scotia Sea, Southern Ocean. Geophys. Res. Lett. 2014GL062744. doi:10.1002/2014GL062744

Checkley, D.M., Entzeroth, L.C., 1985. Elemental and isotopic fractionation of carbon and nitrogen by marine, planktonic copepods and implications to the marine nitrogen cycle. J. Plankton Res. 7, 553–568. doi:10.1093/plankt/7.4.553

Christaki, U., Lefèvre, D., Georges, C., Colombet, J., Catala, P., Courties, C., Sime-Ngando, T., Blain, S., Obernosterer, I., 2014. Microbial food web dynamics during spring phytoplankton blooms in the naturally iron-fertilized Kerguelen area (Southern Ocean). Biogeosciences 11, 6739–6753. doi:10.5194/bg-11-6739-2014

Coale, K.H., Bruland, K.W., 1985. $^234Th: ^238U$ Disequilibria Within the California Current. Limnol. Oceanogr. 30, 22–33.

Coale, K.H., Johnson, K.S., Chavez, F.P., Buesseler, K.O., Barber, R.T., Brzezinski, M.A., Cochlan, W.P., Millero, F.J., Falkowski, P.G., Bauer, J.E., Wanninkhof, R.H., Kudela, R.M., Altabet, M.A., Hales, B.E., Takahashi, T., Landry, M.R., Bidigare, R.R., Wang, X., Chase, Z., Strutton, P.G., Friederich, G.E., Gorbunov, M.Y., Lance, V.P., Hilting, A.K., Hiscock, M.R., Demarest, M., Hiscock, W.T., Sullivan, K.F., Tanner, S.J., Gordon, R.M., Hunter, C.N., Elrod, V.A., Fitzwater, S.E., Jones, J.L., Tozzi, S., Koblizek, M., Roberts, A.E., Herndon, J., Brewster, J., Ladizinsky, N., Smith, G., Cooper, D., Timothy, D., Brown, S.L., Selph, K.E., Sheridan, C.C., Twining, B.S., Johnson, Z.I., 2004. Southern Ocean Iron Enrichment Experiment: Carbon Cycling in High- and Low-Si Waters. Science 304, 408–414. doi:10.1126/science.1089778

Coppola, L., Roy-Barman, M., Wassmann, P., Mulsow, S., Jeandel, C., 2002. Calibration of sediment traps and particulate organic carbon export using 234Th in the Barents Sea. Mar. Chem. 80, 11–26. doi:10.1016/S0304-4203(02)00071-3

Davison, P.C., Checkley Jr., D.M., Koslow, J.A., Barlow, J., 2013. Carbon export mediated by mesopelagic fishes in the northeast Pacific Ocean. Prog. Oceanogr. 116, 14–30. doi:10.1016/j.pocean.2013.05.013

De Baar, H.J.W., Boyd, P.W., Coale, K.H., Landry, M.R., Tsuda, A., Assmy, P., Bakker, D.C.E., Bozec, Y., Barber, R.T., Brzezinski, M.A., Buesseler, K.O., Boyé, M., Croot, P.L., Gervais, F., Gorbunov, M.Y., Harrison, P.J., Hiscock, W.T., Laan, P., Lancelot, C., Law, C.S., Levasseur, M., Marchetti, A., Millero, F.J., Nishioka, J., Nojiri, Y., van Oijen, T., Riebesell, U., Rijkenberg, M.J.A., Saito, H., Takeda, S., Timmermans, K.R., Veldhuis, M.J.W., Waite, A.M., Wong, C.-S., 2005. Synthesis of iron fertilization experiments: From the Iron Age in the Age of Enlightenment. J. Geophys. Res. Oceans 110, C09S16. doi:10.1029/2004JC002601

De Baar, H.J.W., Buma, A.G.J., Nolting, R.F., Cadée, G.C., Jacques, G., Tréguer, P., 1990. On iron limitation of the Southern Ocean: experimental observations in the Weddell and Scotia Seas. Mar. Ecol. Prog. Ser. 65, 105–122. doi:doi:10.3354/meps065105

Dilling, L., Alldredge, A.L., 2000. Fragmentation of marine snow by swimming macrozooplankton: A new process impacting carbon cycling in the sea. Deep Sea Res. Part Oceanogr. Res. Pap. 47, 1227–1245. doi:10.1016/S0967-0637(99)00105-3

Dunne, J.P., Sarmiento, J.L., Gnanadesikan, A., 2007. A synthesis of global particle export from the surface ocean and cycling through the ocean interior and on the seafloor. Glob. Biogeochem. Cycles 21, GB4006. doi:10.1029/2006GB002907

Ebersbach, F., Trull, T.W., 2008. Sinking particle properties from polyacrylamide gels during the KErguelen Ocean and Plateau compared Study (KEOPS): Zooplankton control of carbon export in an area of

657 persistent natural iron inputs in the Southern Ocean. Limnol. Oceanogr. 53, 212–224.
658 doi:10.4319/lo.2008.53.1.0212
659 Ebersbach, F., Trull, T.W., Davies, D.M., Bray, S.G., 2011. Controls on mesopelagic particle fluxes in the Sub-
660 Antarctic and Polar Frontal Zones in the Southern Ocean south of Australia in summer—Perspectives
661 from free-drifting sediment traps. Deep Sea Res. Part II Top. Stud. Oceanogr. 58, 2260–2276.
662 doi:10.1016/j.dsr2.2011.05.025
663 Fischer, G., Ratmeyer, V., Wefer, G., 2000. Organic carbon fluxes in the Atlantic and the Southern Ocean:
664 relationship to primary production compiled from satellite radiometer data. Deep Sea Res. Part II Top.
665 Stud. Oceanogr. 47, 1961–1997. doi:10.1016/S0967-0645(00)00013-8
666 Francois, R., Honjo, S., Krishfield, R., Manganini, S., 2002. Factors controlling the flux of organic carbon to the
667 bathypelagic zone of the ocean. Glob. Biogeochem. Cycles 16, 1087. doi:10.1029/2001GB001722
668 Gall, M.P., Strzepek, R., Maldonado, M., Boyd, P.W., 2001. Phytoplankton processes. Part 2: Rates of primary
669 production and factors controlling algal growth during the Southern Ocean Iron RElease Experiment
670 (SOIREE). Deep Sea Res. Part II Top. Stud. Oceanogr., The Southern Ocean Iron Release Experiment
671 (SOIREE) 48, 2571–2590. doi:10.1016/S0967-0645(01)00009-1
672 Gehlen, M., Bopp, L., Emprin, N., Aumont, O., Heinze, C., Ragueneau, O., 2006. Reconciling surface ocean
673 productivity, export fluxes and sediment composition in a global biogeochemical ocean model.
674 Biogeosciences 3, 521–537. doi:10.5194/bg-3-521-2006
675 Gerber, R.P., Gerber, M.B., 1979. Ingestion of natural particulate organic matter and subsequent assimilation,
676 respiration and growth by tropical lagoon zooplankton. Mar. Biol. 52, 33–43. doi:10.1007/BF00386855
677 Giering, S.L.C., Sanders, R., Lampitt, R.S., Anderson, T.R., Tamburini, C., Boutrif, M., Zubkov, M.V., Marsay,
678 C.M., Henson, S.A., Saw, K., Cook, K., Mayor, D.J., 2014. Reconciliation of the carbon budget in the
679 ocean/'s twilight zone. Nature 507, 480–483. doi:10.1038/nature13123
680 Gilman, D.L., Fuglister, F.J., Mitchell, J.M., 1963. On the Power Spectrum of "Red Noise." J. Atmospheric Sci.
681 20, 182–184. doi:10.1175/1520-0469(1963)020<0182:OTPSON>2.0.CO;2
682 Gordon, H.R., McCluney, W.R., 1975. Estimation of the depth of sunlight penetration in the sea for remote
683 sensing. Appl. Opt. 14, 413–416.
684 Gruber, N., Gloor, M., Mikaloff Fletcher, S.E., Doney, S.C., Dutkiewicz, S., Follows, M.J., Gerber, M.,
685 Jacobson, A.R., Joos, F., Lindsay, K., Menemenlis, D., Mouchet, A., Müller, S.A., Sarmiento, J.L.,
686 Takahashi, T., 2009. Oceanic sources, sinks, and transport of atmospheric CO2. Glob. Biogeochem.
687 Cycles 23, GB1005. doi:10.1029/2008GB003349
688 Guidi, L., Jackson, G.A., Stemmann, L., Miquel, J.C., Picheral, M., Gorsky, G., 2008. Relationship between
689 particle size distribution and flux in the mesopelagic zone. Deep Sea Res. Part Oceanogr. Res. Pap. 55,
690 1364–1374. doi:10.1016/j.dsr.2008.05.014
691 Gustafsson, O., Andersson, P., Roos, P., Kukulska, Z., Broman, D., Larsson, U., Hajdu, S., Ingri, J., 2004.
692 Evaluation of the collection efficiency of upper ocean sub-photic-layer sediment traps: A 24-month in
693 situ calibration in the open Baltic Sea using 234Th. Limnol. Oceanogr. Methods 2, 62–74.
694 doi:10.4319/lom.2004.2.62
695 Hawley, N., 1988. Flow in Cylindrical Sediment Traps. J. Gt. Lakes Res. 14, 76–88. doi:10.1016/S0380-
696 1330(88)71534-8
697 Henson, S.A., Sanders, R., Madsen, E., 2012. Global patterns in efficiency of particulate organic carbon export
698 and transfer to the deep ocean. Glob. Biogeochem. Cycles 26, GB1028. doi:10.1029/2011GB004099
699 Henson, S.A., Sanders, R., Madsen, E., Morris, P.J., Le Moigne, F., Quartly, G.D., 2011. A reduced estimate of
700 the strength of the ocean's biological carbon pump. Geophys. Res. Lett. 38, L04606.
701 doi:10.1029/2011GL046735
702 Henson, S.A., Yool, A., Sanders, R., 2014. Variability in efficiency of particulate organic carbon export: A
703 model study. Glob. Biogeochem. Cycles 29, GB4965. doi:10.1002/2014GB004965
704 Hiscock, W.T., Millero, F.J., 2005. Nutrient and carbon parameters during the Southern Ocean iron experiment
705 (SOFeX). Deep Sea Res. Part Oceanogr. Res. Pap. 52, 2086–2108. doi:10.1016/j.dsr.2005.06.010
706 Honjo, S., Francois, R., Manganini, S., Dymond, J., Collier, R., 2000. Particle fluxes to the interior of the
707 Southern Ocean in the Western Pacific sector along 170°W. Deep Sea Res. Part II Top. Stud. Oceanogr.
708 47, 3521–3548. doi:10.1016/S0967-0645(00)00077-1
709 Honjo, S., Manganini, S.J., Krishfield, R.A., Francois, R., 2008. Particulate organic carbon fluxes to the ocean
710 interior and factors controlling the biological pump: A synthesis of global sediment trap programs since
711 1983. Prog. Oceanogr. 76, 217–285. doi:10.1016/j.pocean.2007.11.003
712 Hudson, J.M., Steinberg, D.K., Sutton, T.T., Graves, J.E., Latour, R.J., 2014. Myctophid feeding ecology and
713 carbon transport along the northern Mid-Atlantic Ridge. Deep Sea Res. Part Oceanogr. Res. Pap. 93,
714 104–116. doi:10.1016/j.dsr.2014.07.002
715 Jacquet, S.H.M., Dehairs, F., Savoye, N., Obernosterer, I., Christaki, U., Monnin, C., Cardinal, D., 2008.
716 Mesopelagic organic carbon remineralization in the Kerguelen Plateau region tracked by biogenic

particulate Ba. Deep Sea Res. Part II Top. Stud. Oceanogr. 55, 868–879. doi:10.1016/j.dsr2.2007.12.038
JGOFS Sediment Trap Methods, 1994, in: Protocols for the Joint Global Ocean Flux Study (JGOFS) Core Measurements. Intergovernmental Oceanographic Commission, Scientific Committee on Oceanic Research Manual and Guides, UNESCO, pp. 157–164.
Jouandet, M.P., Blain, S., Metzl, N., Brunet, C., Trull, T.W., Obernosterer, I., 2008. A seasonal carbon budget for a naturally iron-fertilized bloom over the Kerguelen Plateau in the Southern Ocean. Deep Sea Res. Part II Top. Stud. Oceanogr., KEOPS: Kerguelen Ocean and Plateau compared Study 55, 856–867. doi:10.1016/j.dsr2.2007.12.037
Jouandet, M.-P., Jackson, G.A., Carlotti, F., Picheral, M., Stemmann, L., Blain, S., 2014. Rapid formation of large aggregates during the spring bloom of Kerguelen Island: observations and model comparisons. Biogeosciences 11, 4393–4406. doi:10.5194/bg-11-4393-2014
Jouandet, M.-P., Trull, T.W., Guidi, L., Picheral, M., Ebersbach, F., Stemmann, L., Blain, S., 2011. Optical imaging of mesopelagic particles indicates deep carbon flux beneath a natural iron-fertilized bloom in the Southern Ocean. Limnol. Oceanogr. 56, 1130–1140. doi:10.4319/lo.2011.56.3.1130
Karleskind, P., Lévy, M., Memery, L., 2011. Subduction of carbon, nitrogen, and oxygen in the northeast Atlantic. J. Geophys. Res. Oceans 116, C02025. doi:10.1029/2010JC006446
Kohfeld, K.E., Quéré, C.L., Harrison, S.P., Anderson, R.F., 2005. Role of Marine Biology in Glacial-Interglacial CO2 Cycles. Science 308, 74–78. doi:10.1126/science.1105375
Korb, R.E., Whitehouse, M., 2004. Contrasting primary production regimes around South Georgia, Southern Ocean: large blooms versus high nutrient, low chlorophyll waters. Deep Sea Res. Part Oceanogr. Res. Pap. 51, 721–738. doi:10.1016/j.dsr.2004.02.006
Koubbi, P., Duhamel, G., Hebert, C., 2001. Seasonal relative abundance of fish larvae inshore at Îles Kerguelen, Southern Ocean. Antarct. Sci. 13, 385–392. doi:10.1017/S0954102001000542
Koubbi, P., Ibanez, F., Duhamel, G., 1991. Environmental influences on spatio-temporal oceanic distribution of ichthyoplankton around the Kerguelen Islands (Southern Ocean). Mar. Ecol. Prog. Ser. 72, 225–238.
Lampitt, R.S., Antia, A.N., 1997. Particle flux in deep seas: regional characteristics and temporal variability. Deep Sea Res. Part Oceanogr. Res. Pap. 44, 1377–1403. doi:10.1016/S0967-0637(97)00020-4
Lampitt, R.S., Boorman, B., Brown, L., Lucas, M., Salter, I., Sanders, R., Saw, K., Seeyave, S., Thomalla, S.J., Turnewitsch, R., 2008. Particle export from the euphotic zone: Estimates using a novel drifting sediment trap, 234Th and new production. Deep Sea Res. Part Oceanogr. Res. Pap. 55, 1484–1502. doi:10.1016/j.dsr.2008.07.002
Lam, P.J., Bishop, J.K.B., 2007. High biomass, low export regimes in the Southern Ocean. Deep Sea Res. Part II Top. Stud. Oceanogr. 54, 601–638. doi:10.1016/j.dsr2.2007.01.013
Lam, P.J., Doney, S.C., Bishop, J.K.B., 2011. The dynamic ocean biological pump: Insights from a global compilation of particulate organic carbon, CaCO3, and opal concentration profiles from the mesopelagic. Glob. Biogeochem. Cycles 25, GB3009. doi:10.1029/2010GB003868
Landry, M.R., Constantinou, J., Latasa, M., Brown, S.L., Bidigare, R.R., Ondrusek, M.E., 2000. Biological response to iron fertilization in the eastern equatorial Pacific (IronEx II). III. Dynamics of phytoplankton growth and microzooplankton grazing. Mar. Ecol. Prog. Ser. 201, 57–72. doi:10.3354/meps201057
Laurenceau-Cornec, E.C., Trull, T.W., Davies, D.M., Bray, S.G., Doran, J., Planchon, F., Carlotti, F., Jouandet, M.-P., Cavagna, A.-J., Waite, A.M., Blain, S., 2015. The relative importance of phytoplankton aggregates and zooplankton fecal pellets to carbon export: insights from free-drifting sediment trap deployments in naturally iron-fertilised waters near the Kerguelen Plateau. Biogeosciences 12, 1007–1027. doi:10.5194/bg-12-1007-2015
Laws, E.A., D'Sa, E., Naik, P., 2011. Simple equations to estimate ratios of new or export production to total production from satellite-derived estimates of sea surface temperature and primary production. Limnol. Oceanogr. Methods 593–601. doi:10.4319/lom.2011.9.593
Laws, E.A., Falkowski, P.G., Smith, W.O., Ducklow, H., McCarthy, J.J., 2000. Temperature effects on export production in the open ocean. Glob. Biogeochem. Cycles 14, 1231–1246. doi:10.1029/1999GB001229
Lefèvre, D., Guigue, C., Obernosterer, I., 2008. The metabolic balance at two contrasting sites in the Southern Ocean: The iron-fertilized Kerguelen area and HNLC waters. Deep Sea Res. Part II Top. Stud. Oceanogr., KEOPS: Kerguelen Ocean and Plateau compared Study 55, 766–776. doi:10.1016/j.dsr2.2007.12.006
Le Moigne, F.A.C., Sanders, R.J., Villa-Alfageme, M., Martin, A.P., Pabortsava, K., Planquette, H., Morris, P.J., Thomalla, S.J., 2012. On the proportion of ballast versus non-ballast associated carbon export in the surface ocean. Geophys. Res. Lett. 39, L15610. doi:10.1029/2012GL052980
Lenton, A., Tilbrook, B., Law, R.M., Bakker, D., Doney, S.C., Gruber, N., Ishii, M., Hoppema, M., Lovenduski, N.S., Matear, R.J., McNeil, B.I., Metzl, N., Mikaloff Fletcher, S.E., Monteiro, P.M.S., Rödenbeck, C.,

Sweeney, C., Takahashi, T., 2013. Sea–air CO2 fluxes in the Southern Ocean for the period 1990–2009. Biogeosciences 10, 4037–4054. doi:10.5194/bg-10-4037-2013

Le Quéré, C., Andres, R.J., Boden, T., Conway, T., Houghton, R.A., House, J.I., Marland, G., Peters, G.P., van der Werf, G.R., Ahlström, A., Andrew, R.M., Bopp, L., Canadell, J.G., Ciais, P., Doney, S.C., Enright, C., Friedlingstein, P., Huntingford, C., Jain, A.K., Jourdain, C., Kato, E., Keeling, R.F., Klein Goldewijk, K., Levis, S., Levy, P., Lomas, M., Poulter, B., Raupach, M.R., Schwinger, J., Sitch, S., Stocker, B.D., Viovy, N., Zaehle, S., Zeng, N., 2013. The global carbon budget 1959–2011. Earth Syst. Sci. Data 5, 165–185. doi:10.5194/essd-5-165-2013

Levy, M., Bopp, L., Karleskind, P., Resplandy, L., Ethe, C., Pinsard, F., 2013. Physical pathways for carbon transfers between the surface mixed layer and the ocean interior. Glob. Biogeochem. Cycles 27, 1001–1012. doi:10.1002/gbc.20092

Lima, I.D., Lam, P.J., Doney, S.C., 2014. Dynamics of particulate organic carbon flux in a global ocean model. Biogeosciences 11, 1177–1198. doi:10.5194/bg-11-1177-2014

Lutz, M.J., Caldeira, K., Dunbar, R.B., Behrenfeld, M.J., 2007. Seasonal rhythms of net primary production and particulate organic carbon flux to depth describe the efficiency of biological pump in the global ocean. J. Geophys. Res. Oceans 112, C10011. doi:10.1029/2006JC003706

Maiti, K., Charette, M.A., Buesseler, K.O., Kahru, M., 2013. An inverse relationship between production and export efficiency in the Southern Ocean. Geophys. Res. Lett. 40, 1557–1561. doi:10.1002/grl.50219

Manno, C., Stowasser, G., Enderlein, P., Fielding, S., Tarling, G.A., 2014. The contribution of zooplankton faecal pellets to deep carbon transport in the Scotia Sea (Southern Ocean). Biogeosciences Discuss 11, 16105–16134. doi:10.5194/bgd-11-16105-2014

Maraldi, C., Lyard, F., Testut, L., Coleman, R., 2011. Energetics of internal tides around the Kerguelen Plateau from modeling and altimetry. J. Geophys. Res. Oceans 116, C06004. doi:10.1029/2010JC006515

Maraldi, C., Mongin, M., Coleman, R., Testut, L., 2009. The influence of lateral mixing on a phytoplankton bloom: Distribution in the Kerguelen Plateau region. Deep Sea Res. Part Oceanogr. Res. Pap. 56, 963–973. doi:10.1016/j.dsr.2008.12.018

Maritorena, S., Siegel, D.A., 2005. Consistent merging of satellite ocean color data sets using a bio-optical model. Remote Sens. Environ. 94, 429–440. doi:10.1016/j.rse.2004.08.014

Martin, J.H., Knauer, G.A., Karl, D.M., Broenkow, W.W., 1987. VERTEX: carbon cycling in the northeast Pacific. Deep Sea Res. Part Oceanogr. Res. Pap. 34, 267–285. doi:10.1016/0198-0149(87)90086-0

Martin, P., van der Loeff, M.R., Cassar, N., Vandromme, P., d' Ovidio, F., Stemmann, L., Rengarajan, R., Soares, M., González, H.E., Ebersbach, F., Lampitt, R.S., Sanders, R., Barnett, B.A., Smetacek, V., Naqvi, S.W.A., 2013. Iron fertilization enhanced net community production but not downward particle flux during the Southern Ocean iron fertilization experiment LOHAFEX. Glob. Biogeochem. Cycles 27, 871–881. doi:10.1002/gbc.20077

Matsuno, K., Yamaguchi, A., Fujiwara, A., Onodera, J., Watanabe, E., Imai, I., Chiba, S., Harada, N., Kikuchi, T., 2014. Seasonal changes in mesozooplankton swimmers collected by sediment trap moored at a single station on the Northwind Abyssal Plain in the western Arctic Ocean. J. Plankton Res. 36, 490–502. doi:10.1093/plankt/fbt092

Measures, C.I., Brown, M.T., Selph, K.E., Apprill, A., Zhou, M., Hatta, M., Hiscock, W.T., 2013. The influence of shelf processes in delivering dissolved iron to the HNLC waters of the Drake Passage, Antarctica. Deep Sea Res. Part II Top. Stud. Oceanogr. 90, 77–88. doi:10.1016/j.dsr2.2012.11.004

Metzl, N., Brunet, C., Jabaud-Jan, A., Poisson, A., Schauer, B., 2006. Summer and winter air–sea CO2 fluxes in the Southern Ocean. Deep Sea Res. Part Oceanogr. Res. Pap. 53, 1548–1563. doi:10.1016/j.dsr.2006.07.006

Moore, J.K., Doney, S.C., Lindsay, K., 2004. Upper ocean ecosystem dynamics and iron cycling in a global three-dimensional model. Glob. Biogeochem. Cycles 18, GB4028. doi:10.1029/2004GB002220

Morales, C.E., 1987. Carbon and nitrogen content of copepod faecal pellets: effect of food concentration and feeding behaviour. Mar. Ecol. Prog. Ser. 36, 107–114.

Obernosterer, I., Christaki, U., Lefèvre, D., Catala, P., Van Wambeke, F., Lebaron, P., 2008. Rapid bacterial mineralization of organic carbon produced during a phytoplankton bloom induced by natural iron fertilization in the Southern Ocean. Deep Sea Res. Part II Top. Stud. Oceanogr. 55, 777–789. doi:10.1016/j.dsr2.2007.12.005

O'Neill, L.P., Benitez-Nelson, C.R., Styles, R.M., Tappa, E., Thunell, R.C., 2005. Diagenetic effects on particulate phosphorus samples collected using formalin poisoned sediment traps. Limnol. Oceanogr. Methods 3, 308–317. doi:10.4319/lom.2005.3.308

Park, Y.-H., Charriaud, E., Pino, D.R., Jeandel, C., 1998. Seasonal and interannual variability of the mixed layer properties and steric height at station KERFIX, southwest of Kerguelen. J. Mar. Syst. 17, 571–586. doi:10.1016/S0924-7963(98)00065-7

836 Park, Y.-H., Fuda, J.-L., Durand, I., Naveira Garabato, A.C., 2008a. Internal tides and vertical mixing over the
837 Kerguelen Plateau. Deep Sea Res. Part II Top. Stud. Oceanogr. 55, 582–593.
838 doi:10.1016/j.dsr2.2007.12.027
839 Park, Y.-H., Roquet, F., Durand, I., Fuda, J.-L., 2008b. Large-scale circulation over and around the Northern
840 Kerguelen Plateau. Deep Sea Res. Part II Top. Stud. Oceanogr. 55, 566–581.
841 doi:10.1016/j.dsr2.2007.12.030
842 Peterson, M.L., Wakeham, S.G., Lee, C., Askea, M.A., Miquel, J.C., 2005. Novel techniques for collection of
843 sinking particles in the ocean and determining their settling rates. Limnol. Oceanogr. Methods 3, 520–
844 532. doi:10.4319/lom.2005.3.520
845 Picheral, M., Guidi, L., Stemmann, L., Karl, D.M., Iddaoud, G., Gorsky, G., 2010. The Underwater Vision
846 Profiler 5: An advanced instrument for high spatial resolution studies of particle size spectra and
847 zooplankton. Limnol. Oceanogr. Methods 8, 462–473. doi:10.4319/lom.2010.8.462
848 Planchon, F., Ballas, D., Cavagna, A.-J., Bowie, A.R., Davies, D., Trull, T., Laurenceau, E., Van Der Merwe, P.,
849 Dehairs, F., 2014. Carbon export in the naturally iron-fertilized Kerguelen area of the Southern Ocean
850 based on the 234Th approach. Biogeosciences Discuss 11, 15991–16032. doi:10.5194/bgd-11-15991-
851 2014
852 Pollard, R., Sanders, R., Lucas, M., Statham, P., 2007. The Crozet Natural Iron Bloom and Export Experiment
853 (CROZEX). Deep Sea Res. Part II Top. Stud. Oceanogr. 54, 1905–1914.
854 doi:10.1016/j.dsr2.2007.07.023
855 Pollard, R.T., Salter, I., Sanders, R.J., Lucas, M.I., Moore, C.M., Mills, R.A., Statham, P.J., Allen, J.T., Baker,
856 A.R., Bakker, D.C.E., Charette, M.A., Fielding, S., Fones, G.R., French, M., Hickman, A.E., Holland,
857 R.J., Hughes, J.A., Jickells, T.D., Lampitt, R.S., Morris, P.J., Nédélec, F.H., Nielsdóttir, M., Planquette,
858 H., Popova, E.E., Poulton, A.J., Read, J.F., Seeyave, S., Smith, T., Stinchcombe, M., Taylor, S.,
859 Thomalla, S., Venables, H.J., Williamson, R., Zubkov, M.V., 2009. Southern Ocean deep-water carbon
860 export enhanced by natural iron fertilization. Nature 457, 577–580. doi:10.1038/nature07716
861 Rembauville, M., Blain, S., Armand, L., Quéguiner, B., Salter, I., 2014. Export fluxes in a naturally fertilized
862 area of the Southern Ocean, the Kerguelen Plateau: ecological vectors of carbon and biogenic silica to
863 depth (Part 2). Biogeosciences Discuss 11, 17089–17150. doi:10.5194/bgd-11-17089-2014
864 Rigual-Hernández, A.S., Trull, T.W., Bray, S.G., Closset, I., Armand, L.K., 2015. Seasonal dynamics in diatom
865 and particulate export fluxes to the deep sea in the Australian sector of the southern Antarctic Zone. J.
866 Mar. Syst. 142, 62–74. doi:10.1016/j.jmarsys.2014.10.002
867 Rivkin, R.B., Legendre, L., 2001. Biogenic carbon cycling in the upper ocean: effects of microbial respiration.
868 Science 291, 2398–2400. doi:10.1126/science.291.5512.2398
869 Rynearson, T.A., Richardson, K., Lampitt, R.S., Sieracki, M.E., Poulton, A.J., Lyngsgaard, M.M., Perry, M.J.,
870 2013. Major contribution of diatom resting spores to vertical flux in the sub-polar North Atlantic. Deep
871 Sea Res. Part Oceanogr. Res. Pap. 82, 60–71. doi:10.1016/j.dsr.2013.07.013
872 Saba, G.K., Steinberg, D.K., 2012. Abundance, Composition, and Sinking Rates of Fish Fecal Pellets in the
873 Santa Barbara Channel. Sci. Rep. 2. doi:10.1038/srep00716
874 Salter, I., Kemp, A.E.S., Lampitt, R.S., Gledhill, M., 2010. The association between biogenic and inorganic
875 minerals and the amino acid composition of settling particles. Limnol. Oceanogr. 55, 2207–2218.
876 doi:10.4319/lo.2010.55.5.2207
877 Salter, I., Kemp, A.E.S., Moore, C.M., Lampitt, R.S., Wolff, G.A., Holtvoeth, J., 2012. Diatom resting spore
878 ecology drives enhanced carbon export from a naturally iron-fertilized bloom in the Southern Ocean.
879 Glob. Biogeochem. Cycles 26, GB1014. doi:10.1029/2010GB003977
880 Salter, I., Lampitt, R.S., Sanders, R., Poulton, A., Kemp, A.E.S., Boorman, B., Saw, K., Pearce, R., 2007.
881 Estimating carbon, silica and diatom export from a naturally fertilised phytoplankton bloom in the
882 Southern Ocean using PELAGRA: A novel drifting sediment trap. Deep Sea Res. Part II Top. Stud.
883 Oceanogr., The Crozet Natural Iron Bloom and Export Experiment CROZEX 54, 2233–2259.
884 doi:10.1016/j.dsr2.2007.06.008
885 Salter, I., Schiebel, R., Ziveri, P., Movellan, A., Lampitt, R., Wolff, G.A., 2014. Carbonate counter pump
886 stimulated by natural iron fertilization in the Polar Frontal Zone. Nat. Geosci. 7, 885–889.
887 doi:10.1038/ngeo2285
888 Sarmiento, J.L., Gruber, N., 2006. Ocean Biogeochemical Dynamics. Princeton University Press, Princeton.
889 Sarmiento, J.L., Le Quéré, C., 1996. Oceanic Carbon Dioxide Uptake in a Model of Century-Scale Global
890 Warming. Science 274, 1346–1350.
891 Sarthou, G., Timmermans, K.R., Blain, S., Tréguer, P., 2005. Growth physiology and fate of diatoms in the
892 ocean: a review. J. Sea Res., Iron Resources and Oceanic Nutrients - Advancement of Global
893 Environmental Simulations 53, 25–42. doi:10.1016/j.seares.2004.01.007

Savoye, N., Benitez-Nelson, C., Burd, A.B., Cochran, J.K., Charette, M., Buesseler, K.O., Jackson, G.A., Roy-Barman, M., Schmidt, S., Elskens, M., 2006. 234Th sorption and export models in the water column: A review. Mar. Chem. 100, 234–249. doi:10.1016/j.marchem.2005.10.014

Savoye, N., Trull, T.W., Jacquet, S.H.M., Navez, J., Dehairs, F., 2008. 234Th-based export fluxes during a natural iron fertilization experiment in the Southern Ocean (KEOPS). Deep Sea Res. Part II Top. Stud. Oceanogr., KEOPS: Kerguelen Ocean and Plateau compared Study 55, 841–855. doi:10.1016/j.dsr2.2007.12.036

Schlitzer, R., 2004. Export production in the Equatorial and North Pacific derived from dissolved oxygen, nutrient and carbon data. J. Oceanogr. Vol 60 No 1 Pp 53–62.

Schulz, M., Mudelsee, M., 2002. REDFIT: estimating red-noise spectra directly from unevenly spaced paleoclimatic time series. Comput. Geosci. 28, 421–426. doi:10.1016/S0098-3004(01)00044-9

Seeyave, S., Lucas, M.I., Moore, C.M., Poulton, A.J., 2007. Phytoplankton productivity and community structure in the vicinity of the Crozet Plateau during austral summer 2004/2005. Deep Sea Res. Part II Top. Stud. Oceanogr., The Crozet Natural Iron Bloom and Export Experiment CROZEX 54, 2020–2044. doi:10.1016/j.dsr2.2007.06.010

Smetacek, V., Assmy, P., Henjes, J., 2004. The role of grazing in structuring Southern Ocean pelagic ecosystems and biogeochemical cycles. Antarct. Sci. 16, 541–558. doi:10.1017/S0954102004002317

Smith, R.C., 1981. Remote sensing and depth distribution of ocean chlorophyll. Mar. Ecol.-Prog. Ser. 5, 359–361.

Tarling, G.A., Ward, P., Atkinson, A., Collins, M.A., Murphy, E.J., 2012. DISCOVERY 2010: Spatial and temporal variability in a dynamic polar ecosystem. Deep Sea Res. Part II Top. Stud. Oceanogr. 59–60, 1–13. doi:10.1016/j.dsr2.2011.10.001

Thomalla, S.J., Fauchereau, N., Swart, S., Monteiro, P.M.S., 2011. Regional scale characteristics of the seasonal cycle of chlorophyll in the Southern Ocean. Biogeosciences 8, 2849–2866. doi:10.5194/bg-8-2849-2011

Trull, T.W., Bray, S.G., Buesseler, K.O., Lamborg, C.H., Manganini, S., Moy, C., Valdes, J., 2008. In situ measurement of mesopelagic particle sinking rates and the control of carbon transfer to the ocean interior during the Vertical Flux in the Global Ocean (VERTIGO) voyages in the North Pacific. Deep Sea Res. Part II Top. Stud. Oceanogr. 55, 1684–1695. doi:10.1016/j.dsr2.2008.04.021

Trull, T.W., Davies, D., Casciotti, K., 2008. Insights into nutrient assimilation and export in naturally iron-fertilized waters of the Southern Ocean from nitrogen, carbon and oxygen isotopes. Deep Sea Res. Part II Top. Stud. Oceanogr. 55, 820–840. doi:10.1016/j.dsr2.2007.12.035

Tsuda, A., Takeda, S., Saito, H., Nishioka, J., Kudo, I., Nojiri, Y., Suzuki, K., Uematsu, M., Wells, M.L., Tsumune, D., Yoshimura, T., Aono, T., Aramaki, T., Cochlan, W.P., Hayakawa, M., Imai, K., Isada, T., Iwamoto, Y., Johnson, W.K., Kameyama, S., Kato, S., Kiyosawa, H., Kondo, Y., Levasseur, M., Machida, R.J., Nagao, I., Nakagawa, F., Nakanishi, T., Nakatsuka, S., Narita, A., Noiri, Y., Obata, H., Ogawa, H., Oguma, K., Ono, T., Sakuragi, T., Sasakawa, M., Sato, M., Shimamoto, A., Takata, H., Trick, C.G., Watanabe, Y.W., Wong, C.S., Yoshie, N., 2007. Evidence for the grazing hypothesis: Grazing reduces phytoplankton responses of the HNLC ecosystem to iron enrichment in the western subarctic pacific (SEEDS II). J. Oceanogr. 63, 983–994. doi:10.1007/s10872-007-0082-x

Uitz, J., Claustre, H., Griffiths, F.B., Ras, J., Garcia, N., Sandroni, V., 2009. A phytoplankton class-specific primary production model applied to the Kerguelen Islands region (Southern Ocean). Deep Sea Res. Part Oceanogr. Res. Pap. 56, 541–560. doi:10.1016/j.dsr.2008.11.006

Villareal, T.A., Adornato, L., Wilson, C., Schoenbaechler, C.A., 2011. Summer blooms of diatom-diazotroph assemblages and surface chlorophyll in the North Pacific gyre: A disconnect. J. Geophys. Res. Oceans 116, C03001. doi:10.1029/2010JC006268

Volk, T., Hoffert, M.I., 1985. Ocean carbon pumps: Analysis of relative strengths and efficiencies in ocean-driven atmospheric CO2 changes, in: Sundquist, E.T., Broecker, W.S. (Eds.), Geophysical Monograph Series. American Geophysical Union, Washington, D. C., pp. 99–110.

944 **Table 1:** Dynamics of carbon and nitrogen export fluxes at station A3 collected by the
945 sediment trap at 289 m.

			Fluxes (mmol m^{-2} d^{-1})			Contribution to annual export (%)	
Cup	**Start**	**Stop**	**POC**	**PON**	**POC:PON**	**POC**	**PON**
1	21/10/2011	04/11/2011	0.15±0.01	0.02±0.00	6.80±0.56	2.11±0.06	2.30±0.01
2	04/11/2011	18/11/2011	0.14 ±0.01	0.02±0.00	6.09±0.67	1.94±0.16	2.27±0.15
3	18/11/2011	02/12/2011	0.15±0.01	0.02±0.00	7.33±0.31	2.12±0.06	1.99±0.06
4	02/12/2011	12/12/2011	1.60±0.04	0.23±0.01	6.95±0.29	16.18±0.45	16.48±0.07
5	12/12/2011	22/12/2011	0.34±0.00	0.05±0.00	6.87±0.08	3.41±0.03	3.64±0.03
6	22/12/2011	01/01/2012	0.51±0.04	0.08±0.01	6.70±0.78	4.82±0.76	5.50±0.39
7	01/01/2012	11/01/2012	0.42±0.02	0.06±0.00	6.73±0.46	4.23±0.14	4.65±0.42
8	11/01/2012	25/01/2012	0.34±0.01	0.05±0.00	6.94±0.38	4.83±0.18	4.84±0.11
9	25/01/2012	08/02/2012	1.47±0.03	0.20±0.01	7.38±0.26	20.98±0.57	21.07±0.05
10	08/02/2012	22/02/2012	0.55±0.04	0.08±0.00	6.97±0.88	7.83±0.64	8.36±0.57
11	22/02/2012	31/05/2012	0.27±0.01	0.03±0.00	8.09±0.22	26.84±0.47	24.12±0.20
12	31/05/2012	07/09/2012	0.04±0.00	0.01±0.00	6.06±0.17	4.71±0.90	4.78±0.09
Annual export (mmol m^{-2} y^{-1})			98.24±4.35	13.59±0.30			

946

947

948 **Table 2:** Number of swimmer individuals found in each cup and swimmer intrusion rate
949 (number d^{-1}, *bold italic* numbers) for each taxa and for the total swimmers.

Cup	Copepod	Pteropod	Euphausiid	Ostracod	Amphipod	Cnidarian	Polychaete	Ctenophore	Siphonophore	Salp	Total
1	166	13	1	2	1	0	0	0	0	0	183
	12	***1***	***< 1***	***< 1***	***< 1***	***0***	***0***	***0***	***0***	***0***	***13***
2	55	0	0	0	0	0	0	0	0	0	55
	4	***0***	***0***	***0***	***0***	***0***	***0***	***0***	***0***	***0***	***4***
3	0	0	0	0	0	0	0	0	0	0	0
	0	***0***	***0***	***0***	***0***	***0***	***0***	***0***	***0***	***0***	***0***
4	113	0	0	0	0	0	0	0	0	0	113
	11	***0***	***0***	***0***	***0***	***0***	***0***	***0***	***0***	***0***	***11***
5	0	0	0	0	0	0	0	0	0	0	0
	0	***0***	***0***	***0***	***0***	***0***	***0***	***0***	***0***	***0***	***0***
6	540	0	1	0	2	5	1	4	1	0	554
	54	***0***	***< 1***	***0***	***< 1***	***< 1***	***0***	***0***	***0***	***0***	***55***
7	583	0	0	0	0	2	2	3	0	0	590
	58	***0***	***0***	***0***	***0***	***< 1***	***< 1***	***< 1***	***0***	***0***	***58***
8	686	33	2	2	8	5	1	4	0	0	741
	49	***2***	***< 1***	***< 1***	***1***	***< 1***	***< 1***	***< 1***	***0***	***0***	***52***
9	392	14	4	3	121	4	2	0	0	0	540
	28	***1***	***< 1***	***< 1***	***9***	***< 1***	***< 1***	***0***	***0***	***0***	***38***
10	264	69	1	2	18	11	0	2	0	0	367
	19	***5***	***< 1***	***< 1***	***1***	***1***	***0***	***< 1***	***0***	***0***	***26***
11	54	0	0	0	29	4	1	0	0	0	88
	1	***0***	***0***	***0***	***< 1***	***< 1***	***< 1***	***0***	***0***	***0***	***1***
12	1481	44	5	7	2	3	2	0	0	1	1544
	15	***< 1***	***< 1***	***< 1***	***< 1***	***< 1***	***< 1***	***0***	***0***	***< 1***	***15***

950

951

952 **Table 3:** Summary of estimates of POC fluxes at the base of, or under, the mixed layer at
953 station A3 from the KEOPS cruises.

Author	Method	Period	Depth (m)	POC flux (mmol m^{-2} d^{-1})
		KEOPS1		
Savoye et al., 2008	^{234}Th deficit	23 Jan – 12 Feb 2005	100	23 ± 3.6
			150	25.7 ± 3.6
			200	24.5 ± 6.8
Ebersbach and Trull, 2008	Drifting gel trap, optical measurements and both constant and power law C conversion factor	4 Feb 2005	200	23.9
		12 Feb 2005	100	5.3
			200	5.2
			330	0.7
			430	1
Jouandet et al., 2008	Annual DIC budget	Annual	MLD base	85
Trull et al., 2008b	Drifting sediment trap	4 Feb 2005	200	7.3-10
		12 Feb 2005		3-3.1
Jouandet et al., 2011	In situ optical measurement (UVP) and power function C conversion factor	22 Jan 2005	200	72.4
			330	27.2
			400	21.6
		23 Jan 2005	200	29.8
			330	26.8
			400	15.9
		12 Feb 2005	200	4.8
			330	5.6
			400	7.9
		KEOPS2		
Planchon et al., 2014	^{234}Th deficit, steady state model	20 Oct 2011	100	3.5 ± 0.9
			150	3.9 ± 0.9
			200	3.7 ± 0.9
		16 Nov 2011	100	4.6 ± 1.5
			150	7.1 ±1.5
			200	3.1 ± 0.6
	^{234}Th deficit, non steady state model	16 Nov 2011	100	7.3 ± 1.8
			150	8.4 ± 1.8
			200	3.8 ± 0.8
Laurenceau-Cornec et al., 2015	Drifting gel trap, optical measurement of particles	16 Nov 2011	210	5.5
	Drifting sediment trap		210	2.2
Jouandet et al., 2014	In situ optical measurement (UVP) and power function C conversion factor	21 Oct 2011	200	0.2
			350	0.1
		16 Nov 2011	200	1.9
			350	0.3

954

Figures captions

Figure 1. Localization of the Kerguelen Plateau in the Indian sector of the Southern Ocean and detailed map of the satellite-derived surface chlorophyll *a* concentration (MODIS level 3 product) averaged over the sediment trap deployment period. Sediment trap location at the A3 station is represented by a black dot, whereas the black circle represents the 100 km radius area used to average the surface chlorophyll *a* time series. Arrows represent surface geostrophic circulation derived from the absolute dynamic topography (AVISO product). Positions of the Antarctic Circumpolar Current core (AAC core), the Polar Front (PF) and the Fawn Through Current (FTC) are shown by thick black arrows. Grey lines are 500 m and 1000 m isobaths.

Figure 2. Schematic of the instrumented mooring line against vertical temperature profiles. The sediment trap and the current meter/CTD sensor location on the mooring line are shown by white circles. Temperature profiles performed during the sediment trap deployment (20 October 2011) are represented by grey lines. Black full line is the median temperature profile from 12 casts realized on the 16 November 2011. Dashed black lines are the first and third quartiles from these casts. The grey rectangle represents the Kerguelen Plateau seafloor. The different water masses are Antarctic Surface Water (AASW), Winter Water (WW) and Upper Circumpolar Deep Water (UCDW).

Figure 3. Hydrological properties recorded by the instrument mooring at station A3. a) depth of the CTD sensor, b) salinity, c) potential temperature, d) line angle, e) current speed, grey lines are raw data, black lines are low-pass filtered data with a Gaussian filter (40 hour window as suggested by the spectral analysis), f) direction and speed of currents represented by vectors (under sampled with a 5 hours interval) and g) wind rose plot of current direction

and intensities, dotted circles are directions relatives frequencies and colors refer to current speed (m s^{-1}).

Figure 4. Potential temperature/salinity diagram at station A3. Data are from the moored CTD (black dots), KEOPS1 (blue line) and KEOPS2 (red line). Grey lines are potential density anomaly. The different water masses are Antarctic Surface Water (AASW), Winter Water (WW) and Upper Circumpolar Deep Water (UCDW).

Figure 5. Power spectrum of the spectral analysis of a) depth time series and b) potential density anomaly time series. Pure red noise (null hypothesis) is represented by red dashed lines for each variable. The period corresponding to a significant power peak (power peak higher than the red noise) is written.

Figure 6. Progressive vector diagram (integration of the current vectors all along the current meter record) calculated from current meter data at 319 m. The color scale refers to date.

Figure 7. Seasonal variations of surface chlorophyll *a* and particulate organic carbon (POC) export. a) Seasonal surface chlorophyll concentration and 16 years climatology (Globcolour) averaged in a 100 km radius around the station A3 station The black line represents the climatology calculated for the period 1997/2013, whilst the green line corresponds to the sediment trap deployment period (2011/2012). b) POC flux (grey bars) and mass percentage of POC (red dotted line). Error bars are standard deviations from triplicates, bold italic numbers refer to cup number.

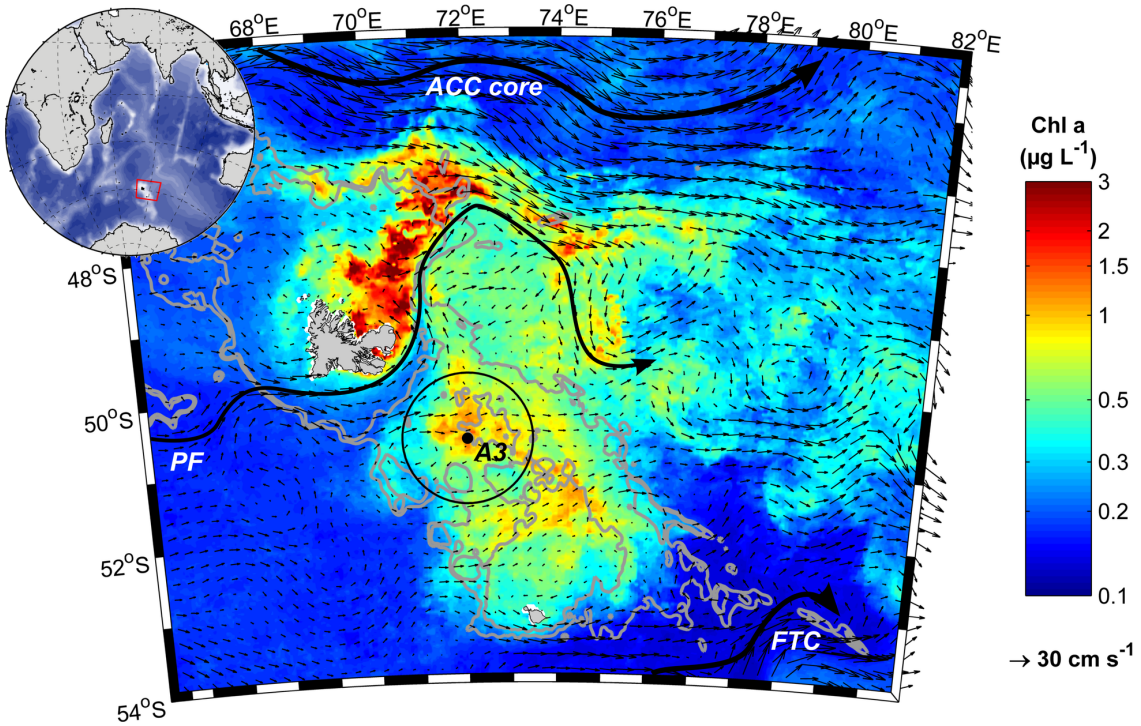

Figure 1.

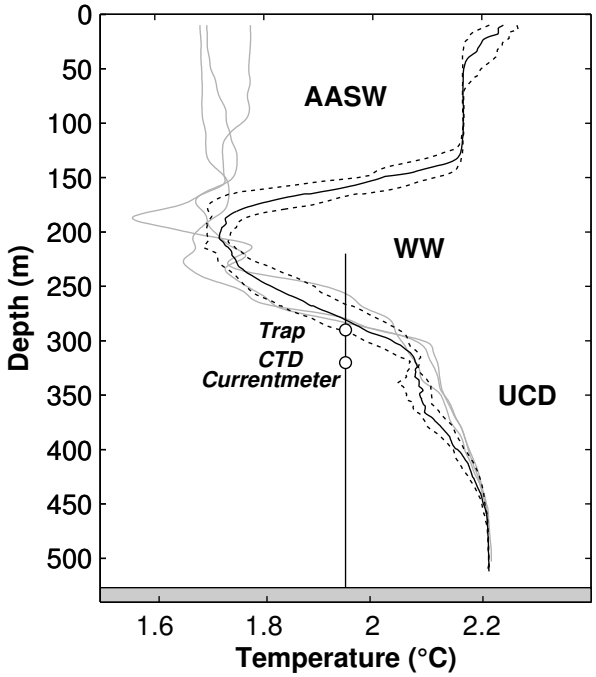

Figure 2.

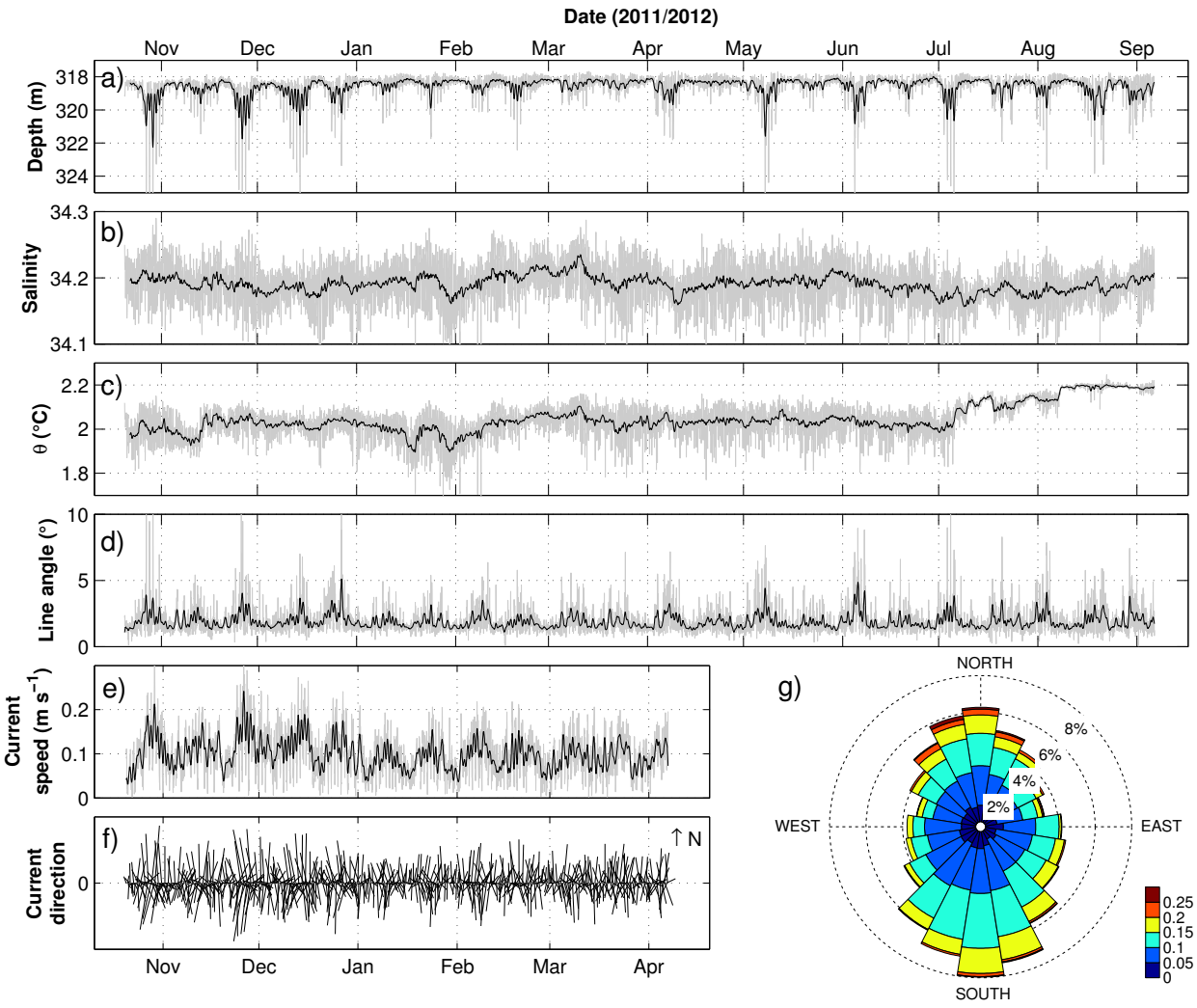
Date (2011/2012)
Nov
Dec
Jan
Feb
Mar
Apr
May
Jun
Jul
Aug
Sep
a)
Depth (m)
318
320
322
324
b)
Salinity
34.3
34.2
34.1
c)
θ (°C)
2.2
2
1.8
d)
Line angle (°)
10
5
0
e)
Current speed (m s^{-1})
0.2
0.1
0
f)
Current direction
0
↑ N
Nov
Dec
Jan
Feb
Mar
Apr
g)
NORTH
8%
6%
4%
2%
WEST
EAST
SOUTH
0.25
0.2
0.15
0.1
0.05
0

Figure 3.

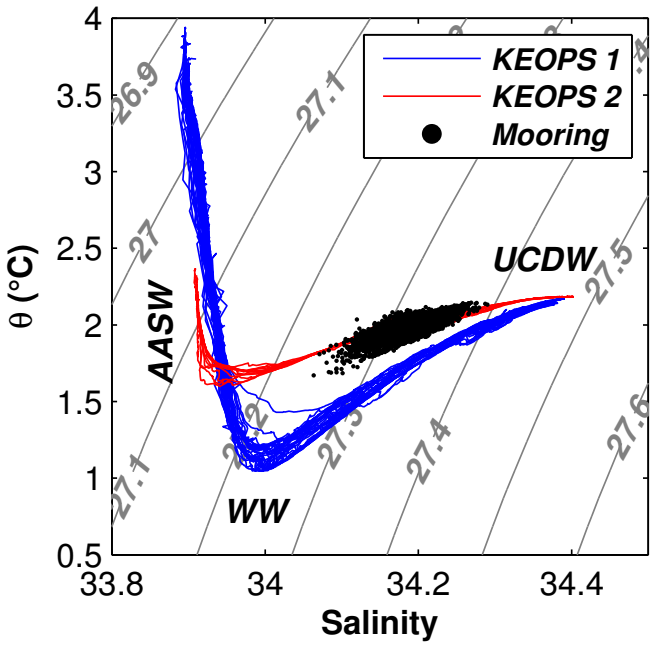

Figure 4.

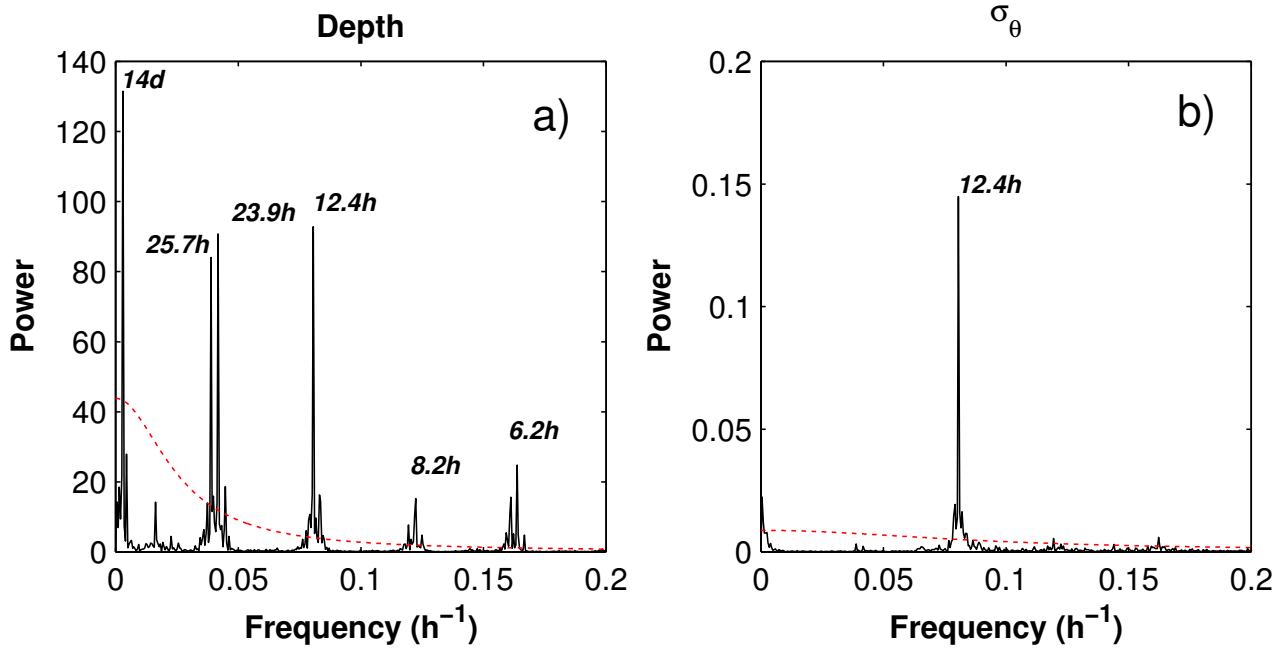

Figure 5.

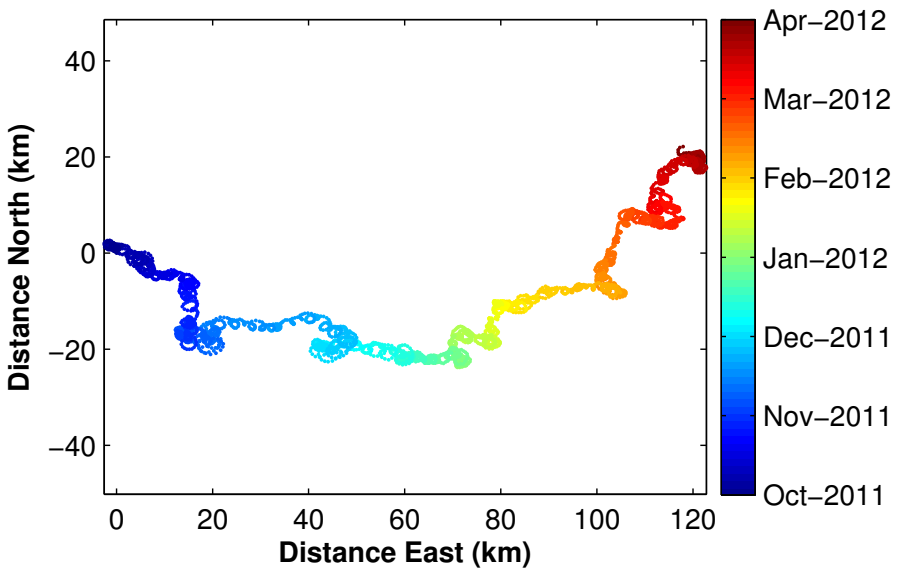

Figure 6.

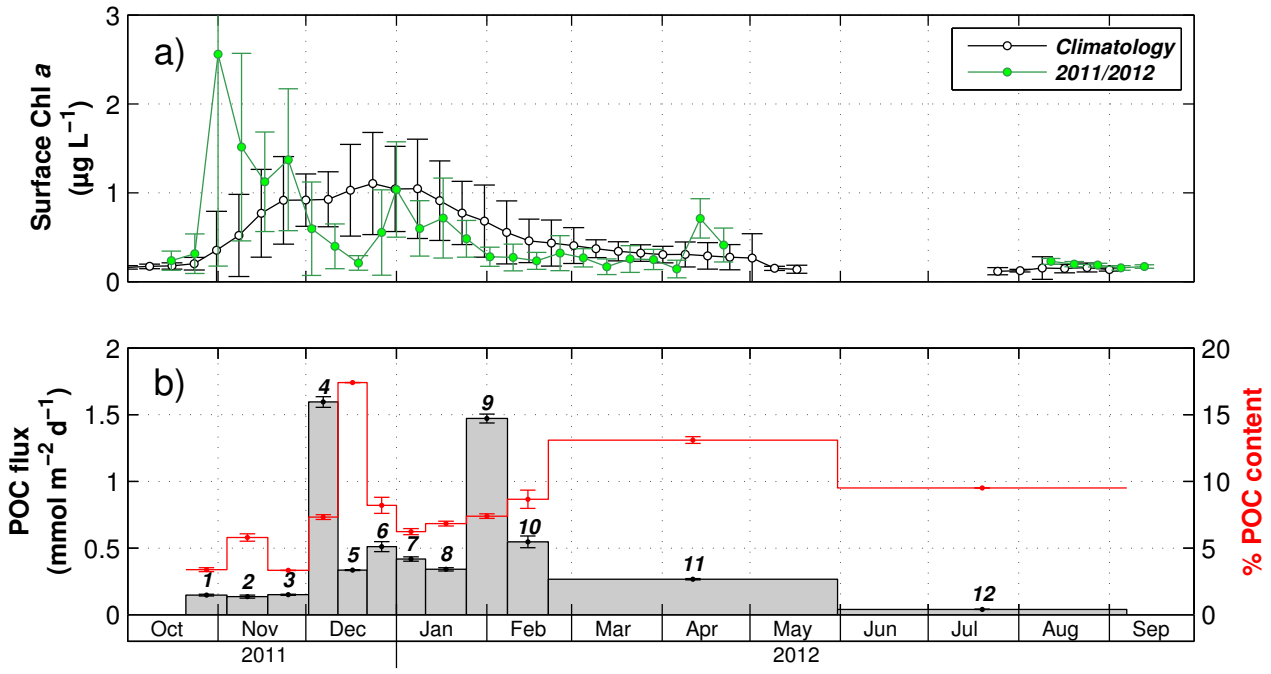

Figure 7.